Fatty acid photodecarboxylase is an ancient photoenzyme that forms hydrocarbons in the thylakoids of algae

Solène Moulin, Audrey Beyly-Adriano, Stéphan Cuiné, Stéphanie Blangy, Bertrand Légeret, Magali Floriani, Adrien Burlacot, Damien Sorigué, Poutoum-Palakiyem Samire, Yonghua Li-Beisson, et al.

Fatty acid photodecarboxylase is an ancient photoenzyme that forms hydrocarbons in the thylakoids of algae

Solène L.Y. Moulin[1], Audrey Beyly-Adriano[1], Stéphan Cuiné[1], Stéphanie Blangy[1], Bertrand Légeret[1], Magali Floriani[2], Adrien Burlacot[1,*], Damien Sorigué[1], Poutoum-Palakiyem Samire[1], Yonghua Li-Beisson[1], Gilles Peltier[1], Fred Beisson[1]

[1]Aix-Marseille University, CEA, CNRS, Institute of Biosciences and Biotechnologies of Aix-Marseille (BIAM), UMR7265, CEA Cadarache, 13108 Saint-Paul-lez-Durance, France.

[2]Institut de Radioprotection et de Sûreté Nucléaire (IRSN), PRP-ENV/SRTE/LECO, Cadarache, 13108 Saint-Paul-Lez-Durance, France.

[*]Present address: Howard Hughes Medical Institute, Department of Plant and Microbial Biology, 111 Koshland Hall, University of California, Berkeley, CA 94720-3102 USA

One sentence summary : **Most algal lineages have the ability to produce hydrocarbons in thylakoids of the chloroplast.** FAP is present in thylakoids and conserved beyond green algae.

Short title: **FAP location, function and biodiversity**

Corresponding author: Fred Beisson
CEA Cadarache, France; Email: frederic.beisson@cea.fr
Tel: +33442252897 Fax: +3344225626

Author Contributions:
F.B. conceived the original research project; F.B., S.M. and G.P. designed the experiments and analyzed the data; S.M., A.B.-A., S.C., S.B., D.S., B.L., A.B., P.S. performed experiments; M.F. performed the TEM study; S.M. performed phylogenetic analysis; F.B. and S.M. wrote the article with contributions from Y.L.-B. and G.P.

This project received funding from CEA (DRF Impulsion Invention E2FAP to F.B.) and from Agence Nationale de la Recherche (PHOTOALKANE, N° ANR-18-CE43-0008-01, to G.P.). This work was also supported by the HelioBiotec platform funded by the EU, the Région Sud, the French Ministry of Research, and the CEA. S.M. has received a PhD scholarship from Ecole Normale Supérieure Paris and the French Ministry of Education and Research.

ABSTRACT

Fatty acid photodecarboxylase (FAP) is one of the few enzymes that require light for their catalytic cycle (photoenzymes). FAP was first identified in the microalga *Chlorella variabilis* NC64A, and belongs to an algae-specific subgroup of the glucose-methanol-choline oxidoreductase family. While the FAP from *C. variabilis* and its *Chlamydomonas reinhardtii* homolog CrFAP have demonstrated *in vitro* activities, their activities and physiological functions have not been studied *in vivo*. Furthermore, the conservation of FAP activity beyond green microalgae remains hypothetical. Here, using a *C. reinhardtii* FAP knockout line (*fap*), we showed that *Cr*FAP is responsible for the formation of 7-heptadecene, the only hydrocarbon of this alga. We further showed that *Cr*FAP was predominantly membrane-associated and that >90% of 7-heptadecene was recovered in the thylakoid fraction. In the *fap* mutant, photosynthetic activity was not affected under standard growth conditions, but was reduced after cold acclimation when light intensity varied. A phylogenetic analysis that included sequences from Tara Ocean identified almost 200 putative FAPs and indicated that FAP was acquired early after primary endosymbiosis. Within Bikonta, FAP was retained in secondary photosynthetic endosymbiosis lineages but absent from those that lost the plastid. Characterization of recombinant FAPs from various algal genera (*Nannochloropsis, Ectocarpus, Galdieria, Chondrus*) provided experimental evidence that FAP photochemical activity was present in red and brown algae, and was not limited to unicellular species. These results thus indicate that FAP was conserved during the evolution of most algal lineages where photosynthesis was retained, and suggest that its function is linked to photosynthetic membranes.

INTRODUCTION

Most organisms have the ability to synthesize highly hydrophobic compounds made only of carbon and hydrogen called hydrocarbons (HCs). Many HCs are isoprenoids but others like *n*-alkanes and their unsaturated analogues (*n*-alkenes) derive from fatty acids (Herman and Zhang, 2016). In plants, C29-C35 *n*-alkanes are synthesized in the epidermis from very-long-chain fatty acids, and secreted onto the surface of aerial organs (Lee and Suh, 2013). Plant *n*-alkanes are important for adaptation to the terrestrial environment because they constitute a major part of the wax layer of the extracellular cuticle that prevents the loss of internal water. Occurrence of *n*-alka(e)nes has also been reported in microorganisms such as microalgae (Sorigué et al., 2016) and cyanobacteria (Schirmer et al., 2010). The magnitude and biogeochemical importance of HC production by marine cyanobacteria (and possibly microalgae) is an intriguing question (Lea-Smith et al., 2015; Valentine and Reddy, 2015). Microbial HCs are presumably mostly located in membranes, but their physiological function has not been studied much. While in cyanobacteria *n*-alka(e)nes have been proposed to play roles in cell growth, cell division, photosynthesis and salt tolerance (Berla et al., 2015; Lea-Smith et al., 2016; Yamamori et al., 2018; Knoot and Pakrasi, 2019), in microalgae the biological function of *n*-alka(e)nes is still completely unknown. Besides the elucidation of their biological roles, *n*-alkanes and *n*-alkenes have also attracted attention because of their interest as fuels, cosmetics, lubricants and as synthons in organic chemistry (Jetter and Kunst, 2008; Jiménez-Díaz et al., 2017). Bio-based alka(e)ne production would be highly desirable to replace part of petroleum-derived HCs, and is currently the focus of intense research efforts (Zhou et al., 2018; Liu and Li, 2020).

A number of *n*-alka(e)ne-forming enzymes has been identified and characterized in the last decade, and it is now clear that conversion of fatty acids to HCs occurs through a variety of reactions and proteins (Herman and Zhang, 2016). Besides, the biosynthetic enzymes involved in the same types of reactions are not conserved across phylogenetic groups. For

instance, it has been shown in bacteria that synthesis of terminal olefins (1-alkenes) occurs through decarboxylation of a saturated long-chain fatty acid, and that this reaction is catalyzed by a cytochrome P450 in *Jeotgalicoccus* spp. (Rude et al., 2011) and by a non-heme iron oxidase in Pseudomonas (Rui et al., 2014). In the bacterium *Micrococcus luteus*, yet another pathway has been discovered, which consists of the head-to-head condensation of fatty acids to form very-long-chain *n*-alkenes with internal double bonds (Beller et al., 2010). Cyanobacterial *n*-alka(e)nes are produced by two distinct pathways (Schirmer et al., 2010; Mendez-Perez et al., 2011), which have been shown to be mutually exclusive (Coates et al., 2014). In insects, a cytochrome P450 oxidative decarbonylase acts on an aldehyde to produce cuticular alka(e)nes (Qiu et al., 2012). The plant pathway producing the very-long-chain *n*-alkanes of the cuticular waxes may also involve an aldehyde intermediate, and is known to require the ECERIFERUM (CER) proteins : CER1 and CER3 (Bernard et al., 2012), which are homologous to the oxygen-dependent membrane class of diiron fatty acid desaturases.

In microalgae, we have shown that C15-C17 *n*-alka(e)nes occur in *Chlorella variabilis* NC64A (named *C. variabilis* from here on), and that they are synthesized through decarboxylation of long-chain fatty acids (Sorigué et al., 2016). A *C. variabilis* protein with a fatty acid decarboxylase activity was then identified as a photoenzyme (Sorigué et al., 2017), a rare type of enzyme that requires photons at each catalytic cycle (Björn, 2015). The *C. variabilis* protein was thus named fatty acid photodecarboxylase (FAP, E.C. 4.1.1.106). It is one of the few photoenzymes discovered so far, the others being the photosystems, DNA photolyases, and light-dependent protochlorophyllide oxidoreductase. FAP belongs to a family of flavoproteins (Sorigué et al., 2017), the glucose-methanol-choline (GMC) oxidoreductases, which includes a large variety of enzymes present in prokaryotic and eukaryotic organisms (Zámocký et al., 2004). FAP activity thus represents an additional type of chemistry in the GMC oxidoreductase family (Sorigué et al., 2017). Molecular phylogenetic analysis has shown that *C. variabilis* FAP

and *Cr*FAP belong to an algal branch of GMC oxidoreductases. However, whether FAP activity is conserved in other algal lineages beyond green algae and whether FAP is indeed responsible for *n*-alka(e)ne formation *in vivo* remain to be demonstrated. Besides, the subcellular location and role of FAP in algal cells have not yet been investigated.

In this work, we isolate and characterize in *C. reinhardtii* an insertional mutant deficient in FAP (*fap* mutant strain). We show that FAP is indeed responsible for the formation of 7-heptadecene, the only fatty acid-derived HC present in this alga. In addition, we provide evidence for a thylakoid localization of *C. reinhardtii* FAP and its alkene product. We also show that growth and photosynthesis are not affected in the knockout under laboratory conditions, but photosynthetic efficiency is impacted under cold conditions when light intensity varies. Finally, we build a large molecular phylogeny of GMC oxidoreductases based on TARA Ocean data and identify almost 200 uncharacterized putative FAP sequences across algal lineages. Experimental evidence demonstrates that FAP photochemical activity is conserved in red and brown algae, and, since it is also present in macroalgae, is not limited to unicellular species.

RESULTS

FAP is responsible for alkene synthesis in *C. reinhardtii*

Chlamydomonas reinhardtii (hereafter named *C. reinhardtii*) has been previously shown to produce 7-heptadecene (C17:1-alkene) from *cis*-vaccenic acid (Sorigué et al., 2016) and to have a FAP homolog that can also perform photodecarboxylation of fatty acids *in vitro* (Sorigué et al., 2017). Although it seemed likely that FAP proteins are indeed responsible for the synthesis of alka(e)nes produced by *C. reinhardtii* and *C. variabilis*, the possibility that the alkenes are formed *in vivo* by another enzyme could not be ruled out. In order to address this issue and investigate the biological role of FAP, a *C. reinhardtii* strain mutated for FAP was isolated from

the *Chlamydomonas* Library Project (CLiP) (Li et al., 2016). This strain showed undetectable levels of FAP protein **(Fig. 1)** and was named *fap-1*. The only fatty acid-derived HC in *C. reinhardtii,* i.e., 7-heptadecene, could not be detected in *fap-1* knockout or in the two other *fap* mutants isolated (**Fig. 1**). After performing nuclear complementation of *fap-1* using the genomic *FAP* gene expressed under the promotor PsaD, 4 independent transformants with different expression levels of *C. reinhardtii* FAP (*Cr*FAP) were isolated (named Cp-1 to -4). In these complemented strains, production of 7-heptadecene was clearly related to FAP amount (**Fig. 1**). These results thus demonstrate that *Cr*FAP is responsible for alkene formation *in vivo* in *C. reinhardtii*. Cp-4 was one of the three complemented strains with 7-heptadecene levels similar to the WT strains used for physiological studies (see Material and Methods for the isolation of the WT, *fap* and *Cp* strains).

FAP activity is conserved beyond green microalgae

Molecular phylogeny of GMC oxidoreductases has previously shown that *Cr*FAP and the FAP from *C. variabilis* (*Cv*FAP) are present in an evolutionary branch containing only sequences from algae (Sorigué et al., 2017). The term "algae" is used here in the classical sense of photosynthetic organisms that have chlorophyll *a* as their primary photosynthetic pigment and lack a sterile covering of cells around the reproductive cells (Lee, 2008). To investigate whether FAP activity has been conserved in algal groups other than green algae, genes encoding putative FAPs from selected algal lineages were cloned and expressed in *E. coli,* and the bacterial HC content was analyzed. Considering the basal position of red algae, we decided to explore FAP activity in Rhodophytes, selecting the microalga *Galdieria sulphuraria* and the macroalga *Chondrus crispus*. For algae deriving from secondary endosymbiosis, we also chose the microalga *Nannochloropsis gaditana* and the macroalga *Ectocarpus silicosus*. When cultivated under light, all *E. coli* strains expressing the various FAPs produced a range of *n*-alkanes and

n-alkenes with different chain lengths (C15 to C17) in various proportions **(Fig. 2A)**. The small amount of HCs detected in *E. coli* cells cultivated under dark was not observed in the non-transformed strain or culture medium, and is thus likely to be due to brief illumination required in the cell treatment process. Interestingly, among the FAPs investigated, we observed some profiles of conversion of *E.coli* fatty acids to HCs that are different from that of *Cv*FAP **(Fig. 2B)**. Taken together, these results therefore show that FAP photoenzymatic activity i) is present in red algae, ii) has been conserved in algae with secondary plastids, iii) is not limited to unicellular algae and iv) is likely to be diverse with respect to fatty acid specificity.

Identification of a reservoir of putative FAPs

To provide a wider picture of the occurrence and evolution of putative FAP photoenzymes within algal groups and to increase the reservoir of FAPs for future biotechnological purposes, a large phylogenetic analysis of GMC oxidoreductases sequences was conducted. We used GMC oxidoreductases retrieved from public databases, from sequenced algal genomes (Blaby-Haas and Merchant, 2019) and from the Tara Ocean project (de Vargas et al., 2015). Tara data gave a unique opportunity to enlarge the FAP dataset with marine algal species that may not be easy to grow under laboratory conditions and whose genomes have not been sequenced. Protein sequences sharing between 50 to 33% of homology with the sequence of *C. variabilis variabilis* FAP were retrieved using Basic Local Alignment Search Tool (BLAST) searches in algal genomes and in the TARA dataset **(Supplemental Tables S1, S2)**. Over 500 putative GMC oxidoreductases were thus identified. Additional putative GMC oxidoreductases from various taxa of the three domains of life were selected from public databases in order to have a representative diversity of the whole GMC oxidoreductase superfamily.

Molecular phylogenetic analysis identified almost 200 sequences of putative GMC oxidoreductases that grouped with the 5 FAPs that have demonstrated biochemical activity

(*Cv*FAP, *Cr*FAP and the four additional FAPs characterized in this study). These sequences constitute a reservoir of putative FAPs. Sequences in this FAP group all belonged to algal species **(Fig. 3, Supplemental Fig. S1)**. Logo sequences built with the putative FAPs exhibited highly conserved patterns, some of which were absent in the other GMC oxidoreductases **(Supplemental Fig. S2).** Interestingly, the residues C432 and R451 of *Cv*FAP active site (Sorigué et al., 2017; Heyes et al., 2020) were strictly conserved, and this feature was specific to the FAP group. It is thus likely that all proteins of this group are genuine FAPs.

Sequences from plants as well as other streptophytes (including charophytes) did not group with algal FAPs **(Fig. 3, Supplemental Fig. S1)**. Absence of FAP in charophytes indicated early loss of FAP function in streptophytes. No putative FAP sequences could be found in cyanobacteria, although this group is highly represented in TARA data (de Vargas et al., 2015). Phylogeny within the FAP branch indicated that red algae (rhodophytes) sequences were the most basal. Interestingly, FAP sequences from secondary endosymbiosis-derived species appeared to be more closely related to FAPs of green algae (chlorophytes) than red algae.

Overall, the putative FAPs that could be identified in algae were present in a variety of algal groups, including stramenopiles (heterokonts), haptophytes and dinophytes. Most eukaryotic algae harbored one putative FAP and no other GMC oxidoreductase, but a few algae contained no FAP and/or several non-FAP GMC oxidoreductases **(Fig. 4)**. Indeed, no putative FAP could be found in the sequenced algal genomes of the glaucocystophyte *Cyanophora paradoxa*; Mamiellophyceae species: *Ostreoccocus* spp., *Micromonas* spp. and *Bathycoccus* spp.; and the diatom *Thalassiosira pseudonana*. Conversely, only a few algal sequences could be found in other branches of the GMC oxidoreductase family. Existence in the diatom *Thalassiosira pseudonana* of a GMC oxidoreductase grouping with bacterial choline dehydrogenase was supported by one sequence from the sequenced genome (Tps-GMC) and

one sequence from Tara (48230190). A Tara sequence annotated as a *Pelagomonas* protein (5166790) also turned out not to be located on the FAP clade. The cryptophyte *Guillardia theta* contained 3 different GMC oxidoreductases in 3 different branches but none of them grouped with FAPs. *Ulva mutabilis* had 11 predicted GMCs, but only one was in the FAP clade. The ten other members of this multigene family of *Ulva* appeared to form a group close to plant GMC oxidoreductases. Although exceptions similar to these probably exist in algal diversity, the general picture is that most algae have only one GMC oxidoreductase and that it groups with the characterized FAP clade in the phylogenetic tree.

C. reinhardtii **FAP binds membranes, and most of its products are found in the thylakoid fraction**

*Cr*FAP is predicted by PredAlgo (Tardif et al., 2012), a software dedicated to the analysis of subcellular targeting sequences in green algae, to be localized to the chloroplast. Consistently, *Cr*FAP is found in a set of 996 proteins proposed to be chloroplastic in *C. reinhardtii* (Terashima et al., 2011). A broader study of putative FAP targeting peptides, also using PredAlgo, indicated that FAPs from various green and red algae were largely predicted to be chloroplastic **(Supplemental Fig. S3)**. In algae with secondary plastids (i.e. containing 3 or 4 membranes), the presence of a signal peptide was consistent with targeting to the ER or chloroplast ER (CER) membrane. Further analysis performed using ASAFind (Gruber et al., 2015), a prediction tool designed to recognize CER targeting motifs in signal peptides, indicated that such a motif was present in *Ectocarpus silicosus* and *Nannochloropsis gaditana*. Taken together, these results suggest that FAP homologs are very likely to be localized to chloroplasts in green algae, in red algae, and also in at least some of the algae that acquired plastids through secondary endosymbiosis.

Since *Cr*FAP is a soluble protein (Sorigué *et al.* 2017) and is predicted to be plastidial, we then sought to determine whether it is a stromal protein with no affinity for membranes or if it has some ability to bind thylakoid membranes. Subcellular fractionation of *C. reinhardtii* cells was therefore performed **(Fig. 5A)**. Most of the FAP protein was found in the total membrane fraction. Thylakoid-enriched membranes were then isolated from whole cells using a sucrose gradient purification procedure **(Fig. 5A)**. Co-purification with thylakoids was performed using the D2 protein (PsbD), a thylakoid membrane protein from the photosystem II (PSII) core complex. The fact that the phosphoribulokinase (PRK), used as a control for stroma, could barely be detected in our thylakoid fraction, indicated the presence of little intact chloroplasts or cells. After the thylakoid purification procedure, the amount of *Cr*FAP still bound to this fraction varied between purifications, but the protein was always detectable. A salt wash experiment confirmed that the *Cr*FAP remaining in the thylakoid fraction was tightly bound to the thylakoids, and thus not likely to be a contaminating stromal protein. When analyzing the percentage of 7-heptadecene in total fatty acids in whole cells versus thylakoid-enriched membranes, a slight but significant enrichment in alkene was found in the thylakoid fraction **(Fig. 5B)**. Most importantly, by using the fatty acid C16:1(3t) as a marker of the thylakoid lipids, it could be estimated that the enrichment in 7-heptadecene corresponds, in fact, to the localization of >90% of this compound to the thylakoid fraction **(Fig. 5C)**. Taken together, these results indicated that *Cr*FAP is a chloroplast-targeted soluble protein that has the ability to bind membranes (including the thylakoid fraction) and whose *n*-alka(e)nes products are mostly associated to the thylakoid fraction.

7-Heptadecene content varies with cell cycle in *C. reinhardtii*

The lack of FAP and HCs in chloroplasts of *C. reinhardtii* did not result in any obvious differences in the overall organization of cells or chloroplasts as seen by transmission electron

microscopy (TEM) **(Supplemental Fig. S4)**. To try to gather clues on FAP function, publicly available FAP transcriptomic data were mined. Transcriptomic data (Zones et al., 2015) shows that FAP has a similar expression pattern as those genes encoding proteins of the photosynthetic apparatus **(Supplemental Fig. S5)**. In order to determine whether FAP product varied with time, we monitored total fatty acids and 7-heptadecene content during a day-night cycle in synchronized *C. reinhardtii* cells. While a constant level of 7-heptadecene representing 0.45% of total fatty acids was found most of the time, a substantial peak (0.7%) was observed before the night (after 12 hours of light), and a steep decrease in 7-heptadecene content relative to total fatty acids occurred at the beginning of the night **(Fig. 6A)**. This decrease in relative 7-heptadecene content was concomitant with cell division, as evidenced by the drop in total fatty acid content per cell that occurred at that time **(Fig. 6B).** Interestingly, the peak in 7-heptadecene **(Fig. 6A)** was not associated with an increase in total FAP amount between 8h and 16h **(Fig. 6C)**.

Fatty acid and membrane lipid compositions differ in the *fap* mutants

Since 7-heptadecene content varied during cell cycle and may thus play a role in cell division, growth of the WT and *fap* strains were analyzed. Growth at 25°C was compared in photoautotrophic conditions (mineral medium (MM)) and in mixotrophic conditions (Tris-acetate-phosphate medium (TAP)). No difference between WT and *fap* could be detected, neither in growth rates nor in cell volumes under these conditions **(Supplemental Fig. S6)**. In addition, no difference between WT and *fap* strains could be observed when cells were grown under various concentrations of sodium chloride **(Supplemental Fig. S7)**. Although the lack of HCs had no effect on growth, fatty acid profiling showed some differences in C16:1(9), C18:1(9), and C18:3(9-12-15) **(Supplemental Fig. S8)**. Synchronized cells also exhibited no growth differences between WT and *fap* strains, but exhibited differences in the dynamics of

some fatty acid species **(Supplemental Fig. S9)**. Changes in fatty acid profiles prompted us to perform a lipidomic analysis by UPLC-MS/MS. Interestingly, this analysis revealed that a limited set of lipid molecular species were significantly different between WT and *fap* and that they were all plastidial lipids belonging to the galactolipid classes digalactosyldiacylglycerol (DGDG) and monogalactosyldiacylglycerol (MGDG) **(Fig. 7 and Supplemental Fig. S10)**. The decrease in the relative content of these galactolipid species appeared to be fully restored by complementation in the case of DGDG but not of MGDG **(Fig. 7)**. Taken together, these results indicate that the lack of 7-heptadecene in the *fap* mutant causes a change in thylakoid lipid composition, which is evidenced by the decrease in the relative content of at least 3 galactolipid species belonging to the DGDG class.

FAP is not strongly associated to photosynthetic complexes, and lack of HCs has no effect on their organization

In cyanobacteria, a role of HCs in photosynthesis has been suggested (Berla et al., 2015) but is controversial (Lea-Smith et al., 2016). In *C. reinhardtii*, there was no difference in the 77K chlorophyll fluorescence spectrum between WT, complementation and *fap* mutant strains, which indicated no major changes in antenna distribution around photosystems **(Supplemental Fig. S11A)**. No difference in photosynthetic efficiency could be detected among WT, complementation and *fap* strains grown under standard laboratory conditions **(Supplemental Fig. S11B)**. Membrane inlet mass spectrometry (MIMS) experiments conducted to quantify O_2 exchange showed no difference in respiration or photosynthesis rates between the two genotypes **(Supplemental Fig. S11C)**. Native electrophoresis of proteins from purified thylakoids and FAP immunodetection revealed that FAP could only be detected at an apparent molecular size of the monomeric FAP **(Fig. 8)**, indicating no strong association with proteins

of photosynthetic complexes. Besides, no difference in organization of photosynthetic complexes between WT and *fap* could be seen on the native protein electrophoresis.

Photosynthesis is affected under light and cold stress in the *fap* mutants

Lack of HCs in the *fap* strain did not cause changes in the photosynthesis activity under standard growth conditions. However, since significant modifications in the composition of membrane lipids could be detected, we explored harsher conditions to further challenge photosynthetic membranes. We chose to investigate chilling temperatures because cold is well-known to affect both membrane physical properties and photosynthesis (Los et al., 2013). Using a multicultivator in turbidostat mode, we first stabilized cultures at 25°C under medium light (200 µmol photons m^{-2} s^{-1}), finding the apparent electron transfer rate (ETR) showed no difference under this condition **(Fig. 9A)**. When cooling down the culture to 15°C and after 3 days of acclimation, both ETR and 77 K chlorophyll fluorescence spectra still showed no differences **(Fig. 9B, Supplemental Fig. S11A)**. However, after one day at a lower light intensity (50 µmol photons $m^{-2}s^{-1}$, 15°C), while the maximal PSII yield was equal for all the strains **(Fig. 9C)**, the ETR was lower for the mutant when measured at high light intensities **(Fig. 9D)**. Interestingly, longer acclimation to this condition (3 days) led to the disappearance of this phenotype. This transient phenotype of the *fap* KO was clearly linked to low temperature because shifting cultures at 25°C from medium light to low light did not result in any difference in maximal PSII yield or ETR among the strains **(Fig. 9E)**.

In order to provide support for a possible link between HCs and cold acclimation, 7-heptadecene content was quantified under various growth temperatures. Relative HC content in WT cells clearly increased under cold conditions **(Fig. 10)**. Enrichment of WT membranes in HC was due to a slower decrease in HC synthesis compared to fatty acid synthesis **(Fig. 10B)**. As expected, an increase in the relative content of polyunsaturated species occurred upon cold

treatment in both WT and *fap* strains **(Supplemental Fig. S12)**, but no difference in the dynamics of fatty acid remodeling was observed between the two strains.

DISCUSSION

Here, we report the isolation and characterization of an insertional *C. reinhardtii* mutant deficient in FAP, and we perform phylogenetic and functional analyses of algal homologs. We show that FAP and the vast majority of its 7-heptadecene product are associated to thylakoid membranes. It is also shown that a gene encoding for a putative FAP is present in most algal lineages and indeed encodes a functional fatty acid photodecarboxylase in some species of red algae, and of secondary algae, including some macroalgae. By studying a FAP knock-out *C. reinhardtii* mutant, we provide evidence that lack of HCs is associated correlated with small changes in galactolipid composition, but has no impact on photosynthesis and growth in *C. reinhardtii* under standard culture conditions. However, in the absence of HCs generated by FAP, the photosynthetic activity is transiently affected during cold acclimation when light intensity varies. The possible significance of these results for algal physiology, as well as FAP function and evolution, are discussed below.

*Cr*FAP localization and regulation in algal cells

Based on the characterization of a *fap* mutant, we first show that *Cr*FAP is responsible for the synthesis of all fatty acid-derived HCs found in *C. reinhardtii* cells **(Fig. 1)**. Our result clearly demonstrates that the fatty acid photodecarboxylase activity measured *in vitro* for *Cr*FAP (Sorigué et al., 2017) is not a promiscuous secondary activity and indeed corresponds to a genuine biological activity, namely the light-driven synthesis of 7-heptadecene from *cis*-vaccenic acid **(Fig. 11)**. Also, the results from the *fap* knockout line demonstrate that no other enzyme is able to synthesize 7-heptadecene in *C. reinhardtii*. Furthermore, the HC production

was found to correspond to the quantity of *Cr*FAP present in complementation lines. Thus, FAP is a limiting factor for 7-heptadecene production *in vivo*, but the lipase(s) that may act upstream of FAP to generate the free *cis*-vaccenic acid does not limit the pathway. This conclusion is consistent with a previous observation that 7-heptadecene is increased 8-fold in *C. reinhardtii* when *Cv*FAP is overexpressed (Yunus et al., 2018).

*Cr*FAP is a soluble protein (Sorigué et al. 2017). Using subcellular fractionation of *C. reinhardtii* cells and anti-CrFAP antibodies, we show here that *Cr*FAP is predominantly found in the total membrane fraction **(Fig. 5A)**. Based on the predicted plastid localization of *Cr*FAP **(Supplemental Fig. S3)** and the fact that the thylakoid fraction harbors >90% of the 7-heptadecene product **(Fig. 5C)**, we propose that *in vivo Cr*FAP is a soluble chloroplastic protein that can bind to and unbind from thylakoid membranes. The capacity of *Cr*FAP to bind to thylakoids is supported by the observation that after the thylakoid purification procedure, a fraction of *Cr*FAP is still tightly bound to this fraction **(Fig. 5A)**. Plastidial localization may be a general feature of FAPs because presence of plastid transit peptides in FAPs seems to be a general rule in green and red algae (for primary plastids) and is also predicted for some secondary endosymbiosis-derived algae **(Supplemental Fig. S3)**.

Concerning the regulation of FAP activity in membranes, it is clear that the peak in 7-heptadecene during the cell cycle **(Fig. 6A)** is not due to an increase in the total amount of FAP protein **(Fig. 6C),** and another mode of regulation of FAP activity must exist. Availability of free fatty acid substrates provided by a lipase acting upstream of FAP is a possibility **(Fig. 11)**. The peak in *Cr*FAP gene expression during the day **(Supplemental Fig. S5)** may correspond to the necessity of a high turnover of the *Cr*FAP protein due to photodamage to the protein. This would be consistent with the idea that *C. variabilis* FAP has a radical-based mechanism (Sorigué et al. 2017), which may be the cause of photoinactivation of the protein (Lakavath et al. 2020) and degradation under excessive light (Moulin et al. 2019).

Role of *Cr*FAP products in membranes

In a work reporting cyanobacterial mutants devoid of fatty acid-derived HCs, it has been suggested that HCs are located in membranes and may play a role in cell division (Lea-Smith et al., 2016). In the proposed cyanobacterial model, integration of HCs into the lipid bilayer would be responsible for membrane flexibility and curvature. HCs may play a similar role in thylakoid membranes of green algae. In light of this connection, it is interesting to note that in *C. reinhardtii*, HC production follows lipid production during cell growth except just before mitosis **(Fig. 6A,B)**. The ratio of HCs to FAMEs decreased at the beginning of night, when cells are dividing, indicating that the extra amount of HCs synthesized before the night must be somehow lost or metabolized during cell division. Simple mechanisms that could explain HC loss during cell division involve enrichment in HCs at breaking points of plastidial membranes before cell division, exclusion from these membranes during division, and/or loss to the gas phase of the culture due to HC volatility **(Supplemental Fig. 5B).**

HCs might thus impact local flexibility of algal plastidial membranes and participate in lipid membrane remodeling during cell division. However, under standard culture conditions, the presence of HCs is apparently not critical for chloroplast structure **(Supplemental Fig. 4),** cell size and cell division rate **(Supplemental Fig. 6)**. A role of cyanobacterial HCs in tolerance to salt stress has also been suggested (Yamamori et al., 2018). In *C. reinhardtii*, contrary to what has been shown in cyanobacteria, no difference could be detected in growth under increasing salt concentrations **(Supplemental Fig. 7)**. One could thus hypothesize that even if HCs are produced in chloroplasts and accumulate in thylakoids, their function might be different from in cyanobacteria. It is also possible that laboratory culture conditions used for *C. reinhardtii* (this study) are far from natural growth conditions where HCs may be necessary.

Alternatively, a compensation mechanism for HC loss may operate differently in *C. reinhardtii* and in cyanobacteria. In *C. reinhardtii*, part of this mechanism may involve changes in membrane lipid composition. Interestingly, lipidomic analysis under standard growth conditions unraveled specific changes in DGDG molecular species **(Fig. 7)** but no other significant differences in other class of lipids **(Supplemental Fig. S8)**. Taken together, these results suggest that in *C. reinhardtii* HCs play no crucial role in cell division and growth under standard conditions. Cells may adapt to a lack of HCs by some changes in the composition of membranes, which could specifically involve some DGDG galactolipids. Alternatively, or in addition to this proposed effect on properties of the membrane lipid phase, it cannot be ruled out that 7-heptadecene may act locally to disrupt or enhance some specific protein-protein interactions, or may play a yet to be defined role, such as acting as a signaling molecule or its precursor **(Fig. 11)**.

The fact that FAP gene expression follows that of photosynthesis genes in day-night cycles, the likely localization of FAP in plastids of green and red algae (as well as in some secondary algae), and the localization of part of FAP and almost all its alkene product in *C. reinhardtii* thylakoids, point toward a role of FAPs in the photosynthetic function of algal cells. This idea is strongly reinforced by the conservation of the FAP-encoding gene in many eukaryotic algae but not in non-photosynthetic protists **(Fig. 3 and Fig. 4)** and in *Polytomella*, an algae that has kept some of its plastidial function but lost photosynthesis (Smith and Lee, 2014). As standard culture conditions did not reveal any photosynthesis phenotype in *C. reinhardtii fap* mutant **(Supplemental Fig. S11)**, more challenging conditions involving colder temperatures and variations in light intensity were tested. These experiments have revealed a difference between WT and *fap* mutant in the photosynthesis activity during acclimation to cold after light intensity varied from medium to low **(Fig. 9)**. This difference could be highlighted under the high-light ETR measurement conditions. Interestingly, colder temperatures were associated with

membrane enrichment in HCs **(Fig. 10)** and fatty acid profiles followed similar variations with temperature in both WT and *fap* strains **(Supplemental Fig. S12)**. Taken together, these observations indicate that adaptations in membrane lipid composition compensate partly for the loss of HCs in standard growth conditions, but not in harsher conditions, such as light intensity variations under cold temperatures.

At temperatures lower than 20°C, it is clear that cell division and FAME production slow down **(Fig. 10B)**. Interestingly, HC production does not follow the same pattern, and increases with decreasing temperatures (except at 8°C). Enrichment of membranes in HCs with decreasing temperatures is consistent with our proposal that HCs are lost during cell division **(Supplemental Fig. S5)**: lower temperature causes reduced division and would hence result in lower HC losses. Whether the sustained production of HC at low temperature is an adaptation mechanism to low temperature or not, remains to be elucidated.

Conservation of FAP in algae

According to molecular phylogeny **(Fig. 3, Fig. 4)**, FAP proteins appear to be specific to algae and highly conserved in many algae species. A noticeable exception is the Mamiellophyceae class of the green algae. Algae is a common denomination that covers photosynthetic eukaryotes which mainly live in aquatic environments. This polyphyletic group includes organisms derived from a first endosymbiosis, as well as organisms derived from a secondary, or even tertiary, endosymbiosis. However, a functional FAP can be found in Chlorophyta (green algae), Rhodophyta (*Chondrus* and *Galdieria*) and Stramenopiles (in the phaeophyceae *Ectocarpus* and the Eustigmatophyceae *Nannochloropsis*), as demonstrated by heterologous expression in *E. coli* of the corresponding identified FAPs **(Fig. 2)**. FAP activity was therefore conserved during secondary endosymbiotic event(s) that gave rise to the red algae lineage. Moreover, FAP activity is not specific to the unicellular state, as FAPs were also functional in

459 the pluricellular algae (macroalgae) *Ectocarpus silicosus* and *Chondrus crispus*. Considering
460 homology of sequences, FAP function is thus expected to be present in most algal phyla,
461 including Haptophyta and Dinophyta. Importantly, some amino acid residues that are likely to
462 be involved in fatty acid substrate stabilization or photocatalysis, such as *Cv*FAP Arg451 or
463 Cys432 (Sorigué et al., 2017; Heyes et al., 2020), are strictly conserved in the 198 putative
464 FAPs **(Supplemental Fig. S2)**. This observation reinforces the idea that all the putative FAPs
465 identified in this work have the ability to photo-produce HCs from fatty acids.

466 FAP neofunctionalization from GMC oxidoreductases may have occurred early during
467 evolution of algae, almost concomitantly with the very first endosymbiosis shared by green and
468 red algae. No GMC could be found in Glaucocystophyta **(Fig. 4)**, which may indicate that this
469 neofunctionalization event has occurred after separation of this group from red and green algae.
470 However, it should be noted that so far only one complete Glaucocystophyta genome is
471 available. Absence of FAP in charophytes **(Supplemental. Fig. 1)** indicates early loss of FAP
472 function in Streptophyta. Phylogenetic analysis indicates that FAPs from secondary
473 endosymbiosis lineages are more closely related to core Chlorophyta than to Rhodophyta. FAP
474 could thus be one of the genes that was inherited from green algae by horizontal gene transfer
475 (Moustafa et al., 2009).

476 Concerning the conservation of FAP activity, it should be noted that some of the FAPs
477 selected for heterologous expression had fatty acid preference profiles different from that of
478 *Cv*FAP **(Fig. 2B)**. For example, while *Cv*FAP converted *E. coli* fatty acids into HCs with a
479 slight preference for C18 over C16 fatty acids, *Chondrus* and *Galdieria* FAPs showed higher
480 preference for C16 over C18, and saturated over unsaturated fatty acids. By contrast,
481 *Ectocarpus* FAP had a strong preference for C16:0 over C16:1 fatty acid, and *Nannochloropsis*
482 *gaditana* FAP preferred unsaturated over saturated chain for both C16 and C18 fatty acids. This
483 indicates that the algal biodiversity is likely to contain FAPs with fatty acid specificities

different from the FAPs of *C. variabilis* and *C. reinhardtii*. FAPs with different properties may be useful for a biobased production of specific HCs, for instance shorter chain semi-volatile HCs for liquid fuels (Moulin et al., 2019).

In conclusion, the results presented here show that FAP activity is conserved beyond green microalgae, and identify a big reservoir of FAPs that may be useful for biotechnological applications. It also provides some important clues for future studies aiming at unravelling the exact role of the FAP photoenzyme in eukaryotic algae.

MATERIALS AND METHODS

Strains and culture conditions

The *fap* mutant and its corresponding wild type strain of *C. reinhardtii* were ordered from the CLiP library (Li et al., 2016). Upon receipt, strains were plated on Tris-acetate-phosphate (TAP) medium and streaked to allow formation of single colonies. For each strain, after 1-week growth in the dark, three single-clone derived colonies were randomly chosen for characterization. Wild type strains are CC-4533 cw15 mt^- for mating type minus and CC-5155 cw15 mt^+ (Jonikas CMJ030 F5 backcross strain) [isolate E8] for mating type plus. Mutant LMJ.RY0402.226794 was used in this study, which is predicted to harbor a first insertional cassette in the coding sequence of Cre12.g514200 which encodes FAP. A second insertion in the line LMJ.RY0402.226794 was predicted in Cre14.g628702. To remove this side mutation, we backcrossed the mutant strain to CC-5155. Analysis of one full tetrad showed 2 progeny strains resistant to paromomycin and which were mutated in *FAP* gene. The region of Cre14.g628702 was amplified by PCR and sequenced for the 4 progeny strains of the tetrad. No insertion was actually found, therefore a potential insertion at this locus was ruled out. Work on mutant strains was conducted on one isolated parental strain with the mutation from LMJ.RY0402.226794, and on two mutants from the backcross with CC-5155 (full tetrad).

These three strains are thereafter named *fap-1*, *fap-2*, and *fap-3*. Wild type (WT) strains were parental strain CC5155 (WT-1) and single colony-derived lines of background strain CC4533 (WT-2, WT-3). The average of the three wild type strains and the average of the three knockout strains are labeled WT and *fap*, respectively. For liquid culture experiments, cells were grown in 24 deep well plates of 25 mL culture, under 100 µmol photons m^{-2} s^{-1} with constant shaking at 25°C. Cells were grown in TAP or minimal medium (MM) (Harris, 1989) for mixotrophic and autotrophic conditions, respectively. Cell growth was followed using a cell counter Multisizer (Beckman Coulter). For the day night cycle experiment, cells were cultivated autotrophically in 1L-photobiorectors in turbidostat mode (Sorigué et al., 2016) (OD_{880nm} at 0.4) under 16 hours of light (40 µmol photons m^{-2} s^{-1}) and 8 hours of dark at 25°C. For photosynthesis analysis, cells were grown autotrophically in 80 mL photobioreactors (multicultivator, Photon Systems Instruments) in turbidostat mode (OD_{680nm} at 0.8). Conditions were 25°C, with medium light intensity (200 µmol photons m^{-2} s^{-1}) or low light intensity (50 µmol photons m^{-2} s^{-1}); or 15°C, with medium or low light intensity. All cultures were performed under ambient air.

Complementation of the *fap* mutants

The construct for complementation of the knockout strain for *FAP* gene was performed using pSL-Hyg vector containing an *AphVII* cassette conferring hygromycin resistance. This vector allowing nuclear transformation was kindly provided by Pr. Steven Ball (University of Lille, France). A WT copy of the *FAP* gene was obtained by PCR of WT genomic DNA. It was cloned into TOPO-XL vector. pSL-Hyg vector and *FAP* gene were digested with *Eco*RV and *Spe*I and ligated. Then, the vector was linearized with *Pvu*I and was electroporated into the *fap* strains. Level of complementation was verified by immunoblot (to assess quantity of protein) and by transmethylation of whole cells (to assess quantity of HCs). The two *fap* mutants from a full

tetrad were complemented. Three complemented strains with HC levels similar to WT were kept for physiological studies (*e.g.* Cp-4 shown in Figure 1).

SDS PAGE and Immunodetection

Cells (10–15 mL) were harvested by centrifugation at 3,000*g* for 2 min. Pellets were then frozen in liquid nitrogen and stored at -80°C until use. Pellets were resuspended in 400 mL 1% (w/v) SDS and then 1.6 mL acetone precooled to -20°C was added. After overnight incubation at -20°C, samples were centrifuged (14,000 rpm, 10 min, 4°C). Supernatant was removed and used for chlorophyll quantification using SAFAS UVmc spectrophotometer (SAFAS). Pellets were resuspended to 1 mg chlorophyll mL^{-1} in LDS in the presence of NuPAGE reducing agent (ThermoFischer), and loaded on 10% (w/v) PAGE Bis-Tris SDS gel. To load equal protein amounts for immunoblot analysis, protein contents were estimated by Coomassie Brilliant Blue staining of the gel using an Odyssey IR Imager (LICOR). After gel electrophoresis, proteins were transferred to nitrocellulose membranes for 75 min at 10 V using a semi-dry set up. Membranes were blocked in TBST with milk 5% (w/v) overnight at 4°C then incubated at room temperature in the presence of the following antibodies: anti-Cyt f, anti-AtpB, anti-PsaD, anti-PsbA, anti-LHCSR3 (Agrisera), or anti-FAP (see below). After 2 hour incubation, primary antibody was removed by rinsing 3 times in TBST, and a peroxidase-coupled secondary antibody was added for at least 1 h. Luminescence was detected with a Gbox imaging system (Syngene).

Production of anti-*Cr*FAP antibodies

A codon-optimized synthetic gene encoding *C. reinhardtii FAP* (Sorigué *et al.* 2017) was cloned into the pLIC7 expression vector, allowing the production of a recombinant FAP fused to TEV-cleavable His-tagged *Escherichia coli* thioredoxin. Production was performed in the *E.*

559 *coli* BL21 Star (DE3) strain initially grown at 37°C in TB medium. Induction was initiated at
560 an OD_{600nm} of 0.8 by adding 0.5 mM isopropyl b-D-thiogalactoside (IPTG), and cultures were
561 then grown at 20°C. Following overnight incubation, cells were centrifuged and protein was
562 purified as described previously (Sorigué *et al.* 2017). Purity of the purified protein was
563 controlled on SDS-PAGE and it was brought to a final concentration of 2 mg mL^{-1} using an
564 Amicon-Ultra device (Millipore). Polyclonal antibodies against FAP were raised in rabbits
565 (ProteoGenix, Schiltigheim, France).
566
567 **Analysis of hydrocarbons and fatty acids**
568 For quantification of HCs, approximately one hundred million cells were pelleted by
569 centrifugation in glass tubes. Transmethylation was conducted by adding 2 mL of methanol
570 containing 5% (v/v) sulfuric acid to the cell pellet. Internal standards (10 µg of hexadecane and
571 20 µg of triheptadecanoylglycerol) were added for quantification. Reaction was carried out for
572 90 min at 85°C in sealed glass tubes. After cooling down, one mL of 0.9% (w/v) NaCl and 500
573 µL of hexane were added to the samples to allow phase separation and recovery of fatty acid
574 methyl esters (FAMEs) and HCs in the hexane phase. Samples were mixed and then centrifuged
575 to allow phase separation. Two µL of the hexane phase was injected in the GC-MS/FID.
576 Analyses were carried out on an Agilent 7890A gas chromatographer coupled to an Agilent
577 5975C mass spectrometer (simple quadrupole). A Zebron 7HG-G007-11 (Phenomenex) polar
578 capillary column (length 30 m, internal diameter 0.25 mm, and film thickness 0.25 mm) was
579 used. Helium carrier gas was at 1 mL min^{-1}. Oven temperature was programmed with an initial
580 2-min hold time at 35°C, a first ramp from 35 to 150°C at 15°C min^{-1}, followed by a 1-min hold
581 time at 170°C then a second ramp from 170 to 240°C at 5°C min^{-1} and a final 2-min hold time
582 at 240°C. The MS was run in full scan over 40 to 350 amu (electron impact ionization at 70

eV), and peaks of FAMEs and HCs were quantified based on the FID signal using the internal standards C17:0 FAME and hexadecane, respectively.

Chlorophyll fluorescence measurements and MIMS analysis

Chlorophyll fluorescence measurements were performed using a pulse amplitude-modulated fluorimeter (Dual-PAM 100) upon 15-min dark-adaptation under continuous stirring. Detection pulses (10 mmol photons m^{-2} s^{-1} blue light) were supplied at a 100-Hz frequency. Basal fluorescence (F_0) was measured in the dark prior to the first saturating flash. Red saturating flashes (6,000 mmol photons m^{-2} s^{-1}, 600 ms) were delivered to measure F_m (in the dark) and $F_{m'}$ (in the light). PSII maximum yields were calculated as $(F_m - F_0)/ F_m$, and PSII yield for each light intensity was measured with a saturating flash after 2 to 3 minutes of illumination and was calculated from $(F_{m'} - F)/F_{m'}$. The apparent electron transfer rate (ETR) was calculated as the product of light intensity and PSII yield. MIMS was used to measure gas exchange as described previously (Burlacot et al., 2018) .

Transmission electron microscopy

Cells were grown photoautotrophically in photobioreactors under 40 µmol photons m^{-2} s^{-1} in turbidostat (OD_{880nm} at 0.4). The algal cells were collected by centrifugation (1,500*g*, 1 min) and were immediately fixed with 2.5% (v/v) glutaraldehyde in 0.1 M, pH 7.4 sodium cacodylate buffer for two days at 4°C. They were then washed by resuspending 5 min in the same buffer for three times. Samples were post-osmicated with 1% (w/v) osmium tetroxyde in cacodylate buffer for 1 h, dehydrated through a graded ethanol series, and finally embedded in monomeric resin Epon 812. All chemicals used for histological preparation were purchased from Electron Microscopy Sciences (Hatfield, USA). Ultra-thin sections for transmission electron microscope (90 nm) were obtained by an ultramicrotome UCT (Leica Microsystems GmbH, Wetzlar,

608 Germany) and mounted on copper grids and examined in a Tecnai G2 Biotwin Electron
609 Microscope (ThermoFisher Scientific FEI, Eindhoven, the Netherlands) using an accelerating
610 voltage of 100 kV and equipped with a CCD camera Megaview III (Olympus Soft imaging
611 Solutions GmbH, Münster, Germany).
612
613 **Isolation of thylakoids and native PAGE**
614 Thylakoids were isolated according to a protocol described previously (Chua *et al.* 1975). All
615 steps were performed on ice or at 4°C with as little light as possible. Briefly, cells were pelleted
616 and resuspended in 8 mL 25 mM HEPES, 5 mM $MgCl_2$, 0.3 M sucrose, pH 7.5 with a protease
617 inhibitor cocktail for plant cell and tissue extracts (Sigma P9599). Cells were disrupted with
618 French press at a pressure of 6000 Psi. Total membranes were collected by centrifugation
619 (1,000*g*, 10 min) and washed first in 5 mM HEPES, 10 mM EDTA, 0.3 M sucrose, pH 7.5 and
620 then in 5 mM HEPES, 10 mM EDTA, 1.8 M sucrose, pH 7.5. Sucrose gradient was 0.5 M
621 sucrose (5 mL), 1.3 M sucrose (2 mL), and 1.8 M sucrose, initially containing thylakoids (5
622 mL). After ultracentrifugation (274,000*g*, 1h), thylakoids were collected at the interface
623 between 0.5 and 1.3 M sucrose. They were washed with 5 mM HEPES, 10 mM EDTA, pH 7.5
624 (with or without 0.5 M NaCl) and resuspended at 1 mg mL^{-1} chlorophyll for subsequent SDS-
625 PAGE analysis. For non-denaturing conditions, thylakoids were resuspended in NativePAGE
626 sample buffer (Life technologies) at 1 mg mL^{-1} chlorophyll, then thylakoids were solubilized
627 for 30 min on ice in the same volume of 1% (w/v) n-Dodecyl-alpha-D-Maltoside, 1% (w/v)
628 digitonine (final concentrations : 0.5 mg mL^{-1} chlorophyll,0.5% (w/v) n-Dodecyl-alpha-D-
629 Maltoside and 0.5% (w/v) digitonine. For each sample, 20 µL were then loaded with 2 µL of
630 G-250 sample additive (Life technologies) on 4-16% (w/v) NativePAGE gels (Life
631 technologies). Cathode running buffer (Life technologies) was supplemented with 0.02% (w/v)
632 G-250 for two-thirds of the migration, and with 0.002% (w/v) G-250 for the remaining third.

633 Annotation of observed bands was done according to a previous publication (Pagliano et al.,
634 2012). For immunoblot analysis, native gel was incubated in Tris Glycine SDS buffer, 10%
635 (v/v) ethanol for 15 min and transferred onto PVDF membrane using XCell II Blot module
636 (25v, 1h). Immunodetection was performed as described above.

637 Based on C16:1(3t) FAME, we determined a factor of enrichment expected for a
638 compound that would be located exclusively within thylakoids (ratio EF=C16:1 (3t) $FAME_{whole\ cells}$ /C16:1 (3t) $FAME_{thylakoids}$). Considering the amount of C17:1 alkene found in thylakoids,
640 we calculated the expected content in whole cells, which equals C17:1 $alk_{thylakoids}$*ratio EF. This
641 calculated value for thylakoids was divided by the value for whole cells that had been
642 determined experimentally, which gives the proportion of C17:1 alkane that is present in
643 thylakoids.

644

645 **Lipidomic analysis by UPLC-MS/MS**

646 Lipid molecular species analysis was done by Ultra Performance Liquid Chromatography
647 coupled with tandem Mass Spectrometry (UPLC-MS/MS). Lipids were first extracted with a
648 modified hot isopropanol method. Briefly, *C. reinhardtii* cells were harvested by centrifugation
649 at 4000 rpm for 2 min in glass tubes. Pellets were immediately resuspended in 1 mL of hot
650 isopropanol (85°C) containing 0.01% (w/v) butylated hydroxytoluene (BHT). Sealed tubes
651 were heated at 85°C for 10 minutes to inactivate lipases. Internal standards were added. Lipids
652 were then extracted in 3 mL methyl tert-butyl ether(MTBE) with a phase separation with
653 1 mL of water. Organic phase was collected and aqueous phase was washed with an additional
654 mL of MTBE. Organic phases were evaporated under a gentle nitrogen stream and resuspended
655 in 500 µL of a mixture of acetonitrile/isopropanol/ammonium acetate 10 mM (65:30:5, v/v/v).
656 Lipid molecular species were analyzed on an ultimate RS 3000 UPLC system (ThermoFisher,
657 Waltham, USA) connected to a quadrupole-time-of-flight (QTOF) 5600 mass spectrometer(AB

Sci ex, Framingham, MA, USA) equipped with a duo-spray ion source operating in positive mode. Lipid extracts were first separated on a Kinetex™ (Kinetex, Atlanta, USA) C182.1×150 mm 1.7 μm column (Phenomenex, Torrance, USA). Two solvent mixtures, acetonitrile-water (60:40, v/v) and isopropanol-acetonitrile (90:10, v/v), both containing 10 mM ammonium formate at pH 3.8, were used as eluents A and B, respectively. A 32-min-long binary gradient elution was performed; eluent B was increased from 27 to 97% in 20 min and the mixture was maintained for 5 min; eluent B was then decreased to 27% and the mixture maintained for another 7 min for column re-equilibration. The flow-rate was 0.3 mL min^{-1} and the column oven temperature was maintained at 45°C. Lipid identification was based on retention time and on mass accuracy peaks from the MS survey scan compared with theoretical masses and fragment ions from MS/MS scan. Relative quantification was achieved with multiquant software (AB Sciex, USA) on the basis of intensity values of extracted masses of the different lipids previously identified. Detector response was normalized by the quantity of FAME previously measured by GC-MS for each sample.

Phylogenetic analysis and logo sequences

The *Cv*FAP protein sequence was used as bait and blasted against different databases using tBLASTn or BLASTp (including NCBI, Phytozome, Fernbase, and Unigene TARA ocean databases). Sequences from the BLAST were pooled with reference sequences from a previous tree of the GMC oxidoreductase superfamily (Zámocký et al., 2004). Alignment of sequences was done with Muscle algorithm (Edgar, 2004) and viewed with Seaview software (Gouy et al., 2010). Selection of conserved sites was done with Gblock. A set of 226 conserved positions were used for tree construction using maximum likelihood algorithm (PhyML, with LG matrix) with 100 replicates for bootstrap analysis. Annotation of the tree was done using annotation data provided by TARA. FAP Logo sequence was based on 35 sequences including at least one

sequence of each taxa from the phylogeny. GMC logo sequence was based on sequences of non-FAP GMC oxidoreductases. Alignment of sequences was done using using Muscle algorithm and viewed with Seaview software. Construction of Logo sequences was done using WebLogo (https://weblogo.berkeley.edu/logo.cgi).

Heterologous expression of FAPs in *E.coli*

Coding sequences of putative FAPs from *Galdieria sulphuraria* **(Supplemental Fig. S13)** and *Nannochloropsis gaditana* **(Supplemental Fig. S14)** were directly amplified from cDNAs obtained by reverse transcription of total RNAs. The FAP homologs from *Galdieria*, *Chondrus* and *Ectocarpus* were codon-optimized and synthesized, then cloned into pLIC07 as described before for *Cv*FAP and *Cr*FAP (Sorigué *et al.* 2017). Potential transit peptides were removed for better expression in *E. coli*, and N-terminal sequences were as follows: GFDRSREFDYVIVGGG for *Galdieria*; SSEAATTYDYIIVGGG for *Chondrus*; LQSVSMKAPAAVASSTYDYIIVGGG *for Nannochloropsis*; SMSVAEEGHKFIIIGGG for *Ectocarpus*. *E. coli* were cultivated in Terrific broth medium at 37°C until OD_{600nm} reached 0.8. Expression was then induced with 0.5 mM IPTG and cultures transferred at 22°C under 100 µmol photons m^{-2} s^{-1}.

77K fluorescence emission spectra

Low temperature spectra were measured on whole cells at 77K using a SAFAS Xenius optical fiber fluorescence spectrophotometer (Dang et al., 2014). 200 µL of light-adapted cell suspension was frozen in a liquid nitrogen bath cryostat. The excitation wavelength used was 440 nm, and detection wavelength ranged from 600 to 800 nm with a 5 nm split. Fluorescence emission spectra were all normalized to the 686 nm signal.

Accession numbers

FAP is referenced under the enzyme classification number E.C. 4.1.1.106. Accession numbers of FAP genes expressed in this study are XP_005842992 (*Chlorella variabilis* NC64A), XP_001703004 (*Chlamydomonas reinhardtii*), CBJ25560 (*Ectocarpus silicosus*) and XP_005714951 (*Chondrus crispus*).

SUPPLEMENTAL DATA

Supplemental Figure S1. Phylogenetic tree of GMC oxidoreductase superfamily.
Supplemental Figure S2. Logo sequences for FAPs and other GMC oxidoreductases.
Supplemental Figure S3 .FAP is predicted to be localized in plastids in many algae
Supplemental Figure S4.Ultrastructure of *C. reinhardtii* wild type and *fap* strains.
Supplemental Figure S5. FAP gene expression during day-night cycle and hypothetical mechanism that may explain HC loss.
Supplemental Figure S6. Growth curves and cell volume of wild type and fap strains.
Supplemental Figure S7. Growth of wild type and *fap* strains using various concentrations of salt.
Supplemental Figure S8. Fatty acid profile in mixotrophic conditions.
Supplemental Figure S9. Variation in the proportion of each fatty acid in total fatty acids during cell cycle.
Supplemental Figure S10. Profiles of major glycerolipid species in WT, *fap* and complementation strains.
Supplemental Figure S11. Photosynthetic activity in *fap* and WT strains.
Supplemental Figure S12. Fatty acid acclimation to cold conditions.
Supplemental Figure S13. Sequence of *Galdieria sulphuraria* FAP deduced from the cDNA cloned.
Supplemental Figure S14. Sequence of *Nannochloropsis gaditana* FAP deduced from the cDNA cloned.
Supplemental Table S1. Multiple alignment of FAP sequences used for the phylogenetic analysis (text file).
Supplemental Table S2. List of GMC oxidoreductases used for the phylogenetic analysis.

ACKNOWLEDGEMENTS

We thank Dr. Olivier Vallon for help with analysis of some sequenced algal genomes and helpful discussions. Thanks are due to Dr. Quentin Carradec and Dr. Patrick Wincker for providing access to TARA sequences and to Dr. Florence Corellou, Dr. Eric Maréchal and Prof. Stefano Caffarri for useful discussions. Help of Dr. Philippe Ortet and Emmanuelle Billon with analysis of TARA sequences is also acknowledged.

FIGURE LEGENDS

Figure 1. FAP level corresponds to the amount of 7-heptadecene in *C. reinhardtii* strains mutated in FAP. A, CrFAP gene structure and site of cassette insertion in *fap* knockout strain. Yellow boxes: exons; grey boxes: untranslated regions; red arrow: antibiotic resistance cassette. **B,** relative content of total fatty-acid derived HCs measured on whole cells; the only fatty acid-derived HC of *C. reinhardtii* is 7-heptadecene (abbreviated as C17:1 alk). Values are mean ± SD of n=3 independent experiments for each strain. nd: not detected. **C,** Immunoblot of total protein extract probed with anti-FAP antibody. **D,** Loading control of the immunoblot (Ponceau staining). B, C and D, WT: wild type strains; *fap*: FAP knockout strains; Cp 1 to 4: strains complemented with *FAP* gene (*fap-1* background);. In panels C and D, each track corresponds to the genotype situated just above in panel B.

Figure 2. Hydrocarbons produced in *E.coli* strains expressing various microalgal FAPs. HC content was analysed by GC- MS after transmethylation of whole cells. Data are means ± SD of n=3 independent cultures. Cv, *Chlorella variabilis* NC64A; Chcr, *Chondrus crispus*; Esi, *Ectocarpus silicosus*; Gsu, *Galdieria sulphuraria*; Nga, *Nannochloropsis gaditana*.; n.d., not detected. A, Amounts of hydrocarbon produced in *E. coli* strains cultivated under light or dark. Empty vector strain was cultivated under light. Blank corresponds to culture medium alone. B, Relative conversion of *E. coli* major fatty acids to corresponding HCs. Data represent the amount of a HC produced under light in a FAP-expressing strain divided by the amount of the fatty acid precursor and by the total amount of HCs.

E. coli strains were cultivated under light or dark. HC content was analysed by GC-MS after transmethylation of whole cells. Data are means ± SD of n=3 independent cultures. Cv, *Chlorella variabilis* NC64A; Chcr, *Chondrus crispus*; Esi, *Ectocarpus silicosus*; Gsu, *Galdieria*

sulphuraria; Nga, *Nannochloropsis gaditana*.; n.d., not detected. **A,** Amounts of HCs produced. Empty vector strain was cultivated under light. Blank corresponds to culture medium alone. **B,** Relative conversion of *E. coli* major fatty acids to corresponding HCs. Data represent the amount of a HC produced under light in a FAP-expressing strain expressing divided by the amount of the corresponding fatty acid precursor and by the total amount of HCs.

Figure 3. Identification of a set of putative FAPs across algal groups. A, Simplified circular tree of GMC oxidoreductases showing the number of putative FAP sequences found in each group of algae. All 198 identified putative FAPs belong to algae and have been found in TARA data (161 FAPs) or in sequenced algal genomes (37 FAPs). The tree was built using maximum likelihood algorithm using GMC oxidoreductases from various kingdoms. Annotations are focused on the branch of putative FAPs; other branches are other GMC oxidoreductases. Branches have been collapsed; full tree is available in Figure S1. **B,** Names of algae species with at least one putative FAP. For most algal groups, the number of species listed in B is lower than that indicated in A because many species from TARA data have no annotation down to the species level. When the biochemical activity of the FAP homolog is demonstrated (Sorigué et al., 2017 or this study), species names are indicated in bold.

Figure 4. Overview of the number of FAP homologs and other GMC oxidoreductases identified in eukaryotic algae and other bikonts. In most groups, there is one FAP and no other GMC oxidoreductase. Remarkable species whose number of FAP or other GMC oxidoreductases depart from this rule are listed individually. Hyphens indicate that no protein could be identified by BLAST searches. A widely accepted phylogeny of the Bikonta is used. The dashed line connects the tree of the Bikonta to the rest of the phylogenetic tree of the

Eukaryotes. Photosynthetic groups or species are colored. Rounds correspond to endosymbiosis: blue round with one black circle, primary endosymbiosis; green and red rounds with two black circles, secondary endosymbiosis; red round with three black circles is for tertiary endosymbiosis in some (not all) Dinophyta; red or green rounds indicate red or green plastid origin, respectively; n: nucleomorph; x: secondary plastid loss.

Figure 5. FAP and its 7-heptadecene product are present in a thylakoid membrane-enriched fraction of *C. reinhardtii*. A, Western blot of protein extracts from whole WT cells before (total) and after centrifugation (supernatant and pellet), and from a thylakoid membrane-enriched fraction without (thyl.) or with (thyl. + NaCl) an additional wash with 0.5 M NaCl. PsbD and PRK are thylakoid and stromal proteins, respectively. Proteins were loaded on a constant chlorophyll basis. B, Relative content in 7-heptadecene and C16:1(3t) fatty acid in whole cells and in the thylakoid fraction (thyl.). The C16:1(3t) fatty acid is almost exclusively present in thylakoids and shown for comparison. Values are mean ± SD of n=4 independent experiments. (*) denote p value < 0.05 in 2-sided Student t-test. C, Estimation of the proportion of total 7-heptadecene present in thylakoids (in green) and elsewhere in the cell (in yellow). Proportion of 7-heptadecene in thylakoids was estimated using C16:1(3t) fatty acid as a thylakoid marker (see Material and Methods for calculation).

Figure 6. Variation of 7-heptadecene compared to total fatty acids during *C. reinhardtii* cell cycle. A, 7-Heptadecene content of cells expressed as a percent of total FAMEs. Values are mean ± SD (n=3 biological replicates). **B,** Total fatty acid and 7-heptadecene content per million cells during cell cycle. Total fatty acids were analyzed as FAMEs by GC-MS. A and B, Data are mean ± SD of n=3 independent cultures. The orange dashed line indicates the end of

day time and the beginning of night time (gray shading). **C,** Immunodedection of FAP during day time. The large Rubisco subunit (RBCL) was used as a loading control.

Figure 7. Identification of lipid molecular species significantly different between *C. reinhardtii* WT and *fap* strains. Relative abundance of glycerolipids was measured by LC-MS/MS analysis of total lipid extracts of whole cells. Only glycerolipid molecular species showing significant differences between WT and *fap* strains are shown here (See supplemental figure S12 for complete results). WT, *fap* and Cp: wild type, FAP knockout and complementation strains respectively. Lipid extracts from the three strains were loaded on a constant total fatty acid basis. Data are mean ± SD of n=9 independent cultures (using three different strains for each of the three genotypes). MGDG34:4-1 is one of the two species of MGDG 34:1 species (which differ by 18:3 fatty acid isomers). Stars indicate significant differences according to a Mann-Whitney U-test at $p<0.05$ (*) or $p<0.01$ (**). Cells were grown in TAP medium, under 80 µmol photons m^{-2} s^{-1} in Erlenmeyers.

Figure 8. Thylakoid purification and immunoblot analysis. A, Purification of *C. reinhardtii* thylakoids using a sucrose density gradient. The thylakoid fraction collected is indicated by an arrow. **B,** Blue native polyacrylamide gel of solubilized proteins (0.5% digitonine, 0.5% α-DM) and corresponding immunodetection. WT: Wild type strain, *fap*: FAP knock out strain. * indicates FAP band. ~~A second, dimensional SDS-PAGE and immunodetection (rightmost blot) did not reveal an association of FAP with higher molecular weight complexes that would have been masked in the 1st dimension BN-PAGE.~~

Figure 9. Photosynthetic acclimation to cold conditions in *C. reinhardtii* WT and *fap* strains. Apparent electron transfer rate (ETR) at various light intensities for cells grown in

photoautotrophic conditions at 25°C (A) and 15°C after 3 days acclimation (B). PSII yield (C) and ETR (D) at 15°C after exposure to lower light for one day (50 µmol photon m^{-2} s^{-1}). E, ETR at 25°C after transition to lower light for one day (50 µmol photon m^{-2} s^{-1}). WT, *fap* and Cp: wild type, FAP knockout and complementation strains respectively. Data are mean ± SD of n=3 independent cultures (corresponding to three different strains for each genotype).

Figure 10. Hydrocarbon production in *C. reinhardtii* WT cells cultivated at low temperatures. A, HC content in cells as percentage of total FAMEs. **B,** Dilution rate of culture medium and production of FAMEs and HCs. For A and B, Cells were grown in TAP medium in photobioreactors in turbidostat mode under 50 µmol photons m^{-2} s^{-1}. HC and fatty acid content were analyzed by GC-MS after transmethylation. Data are mean ± SD of n=3 independent cultures.

Figure 11. Proposed pathway for hydrocarbon formation from fatty acids in *C. reinhardtii* and putative roles. The only fatty acid-derived HC in *C. reinhardtii* (7-heptadecene) is generated from *cis*-vaccenic acid by FAP only when cells are exposed to blue light. The fatty acid precursor must be released from a thylakoid lipid by an unknown lipase. The 7-heptadecene FAP product may play several roles in thylakoid membranes depending on temperature and light conditions.

LITERATURE CITED

Beller HR, Goh E-B, Keasling JD (2010) Genes Involved in Long-Chain Alkene Biosynthesis in *Micrococcus luteus*. Appl Environ Microbiol **76**: 1212

Berla BM, Saha R, Maranas CD, Pakrasi HB (2015) Cyanobacterial Alkanes Modulate Photosynthetic Cyclic Electron Flow to Assist Growth under Cold Stress. Sci Rep. doi: 10.1038/srep14894

Bernard A, Domergue F, Pascal S, Jetter R, Renne C, Faure J-D, Haslam RP, Napier JA, Lessire R, Joubès J (2012) Reconstitution of Plant Alkane Biosynthesis in Yeast Demonstrates That *Arabidopsis* ECERIFERUM1 and ECERIFERUM3 Are Core Components of a Very-Long-Chain Alkane Synthesis Complex. Plant Cell **24**: 3106–3118

Björn LO (2015) Photoactive proteins. Photobiology, The science of light and life, 3rd ed. Springer, New-York, pp 139–150

Blaby-Haas CE, Merchant SS (2019) Comparative and Functional Algal Genomics. Annu Rev Plant Biol **70**: 605–638

Burlacot A, Sawyer A, Cuiné S, Auroy-Tarrago P, Blangy S, Happe T, Peltier G (2018) Flavodiiron-Mediated O2 Photoreduction Links H2 Production with CO2 Fixation during the Anaerobic Induction of Photosynthesis. Plant Physiol **177**: 1639–1649

Coates RC, Podell S, Korobeynikov A, Lapidus A, Pevzner P, Sherman DH, Allen EE, Gerwick L, Gerwick WH (2014) Characterization of cyanobacterial hydrocarbon composition and distribution of biosynthetic pathways. PLoS ONE **9**: e85140

Dang K-V, Plet J, Tolleter D, Jokel M, Cuiné S, Carrier P, Auroy P, Richaud P, Johnson X, Alric J, et al (2014) Combined increases in mitochondrial cooperation and oxygen photoreduction compensate for deficiency in cyclic electron flow in Chlamydomonas reinhardtii. Plant Cell **26**: 3036–3050

Edgar RC (2004) MUSCLE: a multiple sequence alignment method with reduced time and space complexity. BMC Bioinformatics **5**: 113

Gouy M, Guindon S, Gascuel O (2010) SeaView Version 4: A Multiplatform Graphical User Interface for Sequence Alignment and Phylogenetic Tree Building. Molecular Biology and Evolution **27**: 221–224

Gruber A, Rocap G, Kroth PG, Armbrust EV, Mock T (2015) Plastid proteome prediction for diatoms and other algae with secondary plastids of the red lineage. Plant J **81**: 519–528

Harris EH (1989) The Chlamydomonas Sourcebook. A Comprehensive Guide to Biology and Laboratory Use. Academic Press, San Diego

Herman NA, Zhang W (2016) Enzymes for fatty acid-based hydrocarbon biosynthesis. Current Opinion in Chemical Biology **35**: 22–28

Heyes DJ, Lakavath B, Hardman SJO, Sakuma M, Hedison TM, Scrutton NS (2020) Photochemical Mechanism of Light-Driven Fatty Acid Photodecarboxylase. ACS Catal **10**: 6691–6696

Jetter R, Kunst L (2008) Plant surface lipid biosynthetic pathways and their utility for metabolic engineering of waxes and hydrocarbon biofuels. Plant J **54**: 670–683

Jiménez-Díaz L, Caballero A, Pérez-Hernández N, Segura A (2017) Microbial alkane production for jet fuel industry: motivation, state of the art and perspectives. Microb Biotechnol **10**: 103–124

Knoot CJ, Pakrasi HB (2019) Diverse hydrocarbon biosynthetic enzymes can substitute for olefin synthase in the cyanobacterium Synechococcus sp. PCC 7002. Sci Rep. doi: 10.1038/s41598-018-38124-y

Lakavath B, Hedison TM, Heyes DJ, Shanmugam M, Sakuma M, Hoeven R, Tilakaratna V, Scrutton NS (2020) Radical-based photoinactivation of fatty acid photodecarboxylases. Anal Biochem. **600**:113749.

Lea-Smith DJ, Biller SJ, Davey MP, Cotton CAR, Perez Sepulveda BM, Turchyn AV, Scanlan DJ, Smith AG, Chisholm SW, Howe CJ (2015) Contribution of cyanobacterial alkane production to the ocean hydrocarbon cycle. Proc Natl Acad Sci U S A **112**: 13591–13596

Lea-Smith DJ, Ortiz-Suarez ML, Lenn T, Nürnberg DJ, Baers LL, Davey MP, Parolini L, Huber RG, Cotton CAR, Mastroianni G, et al (2016) Hydrocarbons Are Essential for Optimal Cell Size, Division, and Growth of Cyanobacteria1[OPEN]. Plant Physiol **172**: 1928–1940

Lee RE (2008) Basic characteristics of the algae. Phycology, 4th ed. Cambridge University Press, New-York, p 3

Lee SB, Suh MC (2013) Recent Advances in Cuticular Wax Biosynthesis and Its Regulation in Arabidopsis. Molecular Plant **6**: 246–249

Li X, Zhang R, Patena W, Gang SS, Blum SR, Ivanova N, Yue R, Robertson JM, Lefebvre PA, Fitz-Gibbon ST, et al (2016) An Indexed, Mapped Mutant Library Enables Reverse Genetics Studies of Biological Processes in Chlamydomonas reinhardtii. The Plant Cell **28**: 367–387

Liu K, Li S (2020) Biosynthesis of fatty acid-derived hydrocarbons: perspectives on enzymology and enzyme engineering. Curr Opin Biotechnol **62**: 7–14

Los DA, Mironov KS, Allakhverdiev SI (2013) Regulatory role of membrane fluidity in gene expression and physiological functions. Photosynth Res **116**: 489–509

Mendez-Perez D, Begemann MB, Pfleger BF (2011) Modular Synthase-Encoding Gene Involved in α-Olefin Biosynthesis in Synechococcus sp. Strain PCC 7002. Appl Environ Microbiol **77**: 4264–4267

Moulin S, Légeret B, Blangy S, Sorigué D, Burlacot A, Auroy P, Li-Beisson Y, Peltier G, Beisson F (2019) Continuous photoproduction of hydrocarbon drop-in fuel by microbial cell factories. Sci Rep. doi: 10.1038/s41598-019-50261-6

Moustafa A, Beszteri B, Maier UG, Bowler C, Valentin K, Bhattacharya D (2009) Genomic footprints of a cryptic plastid endosymbiosis in diatoms. Science **324**: 1724–1726

Pagliano C, Barera S, Chimirri F, Saracco G, Barber J (2012) Comparison of the α and β isomeric forms of the detergent n-dodecyl-D-maltoside for solubilizing photosynthetic complexes from pea thylakoid membranes. Biochim Biophys Acta **1817**: 1506–1515

Qiu Y, Tittiger C, Wicker-Thomas C, Le Goff G, Young S, Wajnberg E, Fricaux T, Taquet N, Blomquist GJ, Feyereisen R (2012) An insect-specific P450 oxidative decarbonylase for cuticular hydrocarbon biosynthesis. Proc Natl Acad Sci USA **109**: 14858–14863

Ritchie RJ (2008) Universal chlorophyll equations for estimating chlorophylls a, b, c, and d and total chlorophylls in natural assemblages of photosynthetic organisms using acetone, methanol, or ethanol solvents. Photosynthetica **46**: 115–126

Rude MA, Baron TS, Brubaker S, Alibhai M, Del Cardayre SB, Schirmer A (2011) Terminal Olefin (1-Alkene) Biosynthesis by a Novel P450 Fatty Acid Decarboxylase from *Jeotgalicoccus* Species. Appl Environ Microbiol **77**: 1718–1727

Rui Z, Li X, Zhu X, Liu J, Domigan B, Barr I, Cate JHD, Zhang W (2014) Microbial biosynthesis of medium-chain 1-alkenes by a nonheme iron oxidase. Proc Natl Acad Sci USA **111**: 18237–18242

Schirmer A, Rude MA, Li X, Popova E, del Cardayre SB (2010) Microbial Biosynthesis of Alkanes. Science **329**: 559–562

Smith DR, Lee RW (2014) A Plastid without a Genome: Evidence from the Nonphotosynthetic Green Algal Genus Polytomella1[W][OPEN]. Plant Physiol **164**: 1812–1819

Sorigué D, Légeret B, Cuiné S, Blangy S, Moulin S, Billon E, Richaud P, Brugière S, Couté Y, Nurizzo D, et al (2017) An algal photoenzyme converts fatty acids to hydrocarbons. Science **357**: 903–907

Sorigué D, Légeret B, Cuiné S, Morales P, Mirabella B, Guédeney G, Li-Beisson Y, Jetter R, Peltier G, Beisson F (2016) Microalgae Synthesize Hydrocarbons from Long-Chain Fatty Acids via a Light-Dependent Pathway. Plant Physiol **171**: 2393

Tardif M, Atteia A, Specht M, Cogne G, Rolland N, Brugière S, Hippler M, Ferro M, Bruley C, Peltier G, et al (2012) PredAlgo: a new subcellular localization prediction tool dedicated to green algae. Mol Biol Evol **29**: 3625–3639

Terashima M, Specht M, Hippler M (2011) The chloroplast proteome: a survey from the Chlamydomonas reinhardtii perspective with a focus on distinctive features. Curr Genet **57**: 151–168

Valentine DL, Reddy CM (2015) Latent hydrocarbons from cyanobacteria. Proc Natl Acad Sci U S A **112**: 13434–13435

de Vargas C, Audic S, Henry N, Decelle J, Mahé F, Logares R, Lara E, Berney C, Le Bescot N, Probert I, et al (2015) Ocean plankton. Eukaryotic plankton diversity in the sunlit ocean. Science **348**: 1261605

Yamamori T, Kageyama H, Tanaka Y, Takabe T (2018) Requirement of alkanes for salt tolerance of Cyanobacteria: characterization of alkane synthesis genes from salt-sensitive Synechococcus elongatus PCC7942 and salt-tolerant Aphanothece halophytica. Lett Appl Microbiol **67**: 299–305

Yunus IS, Wichmann J, Wördenweber R, Lauersen KJ, Kruse O, Jones PR (2018) Synthetic metabolic pathways for photobiological conversion of CO2 into hydrocarbon fuel. Metab Eng **49**: 201–211

Zámocký M, Hallberg M, Ludwig R, Divne C, Haltrich D (2004) Ancestral gene fusion in cellobiose dehydrogenases reflects a specific evolution of GMC oxidoreductases in fungi. Gene **338**: 1–14

Zhou YJ, Kerkhoven EJ, Nielsen J (2018) Barriers and opportunities in bio-based production of hydrocarbons. Nature Energy **3**: 925–935

Zones JM, Blaby IK, Merchant SS, Umen JG (2015) High-Resolution Profiling of a Synchronized Diurnal Transcriptome from Chlamydomonas reinhardtii Reveals Continuous Cell and Metabolic Differentiation. Plant Cell **27**: 2743–2769

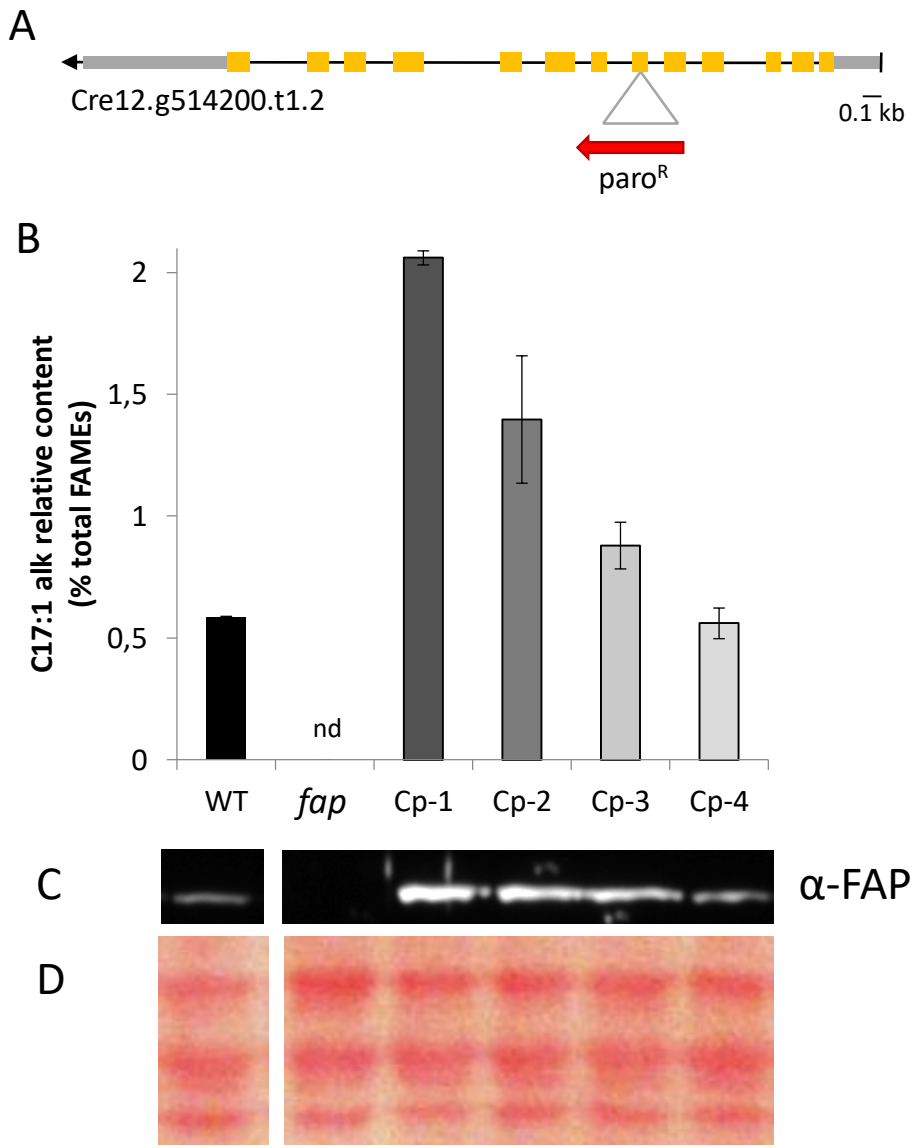
A
Cre12.g514200.t1.2
0.1 kb
paroR
B
C17:1 alk relative content (% total FAMEs)
2
1,5
1
0,5
0
nd
WT
fap
Cp-1
Cp-2
Cp-3
Cp-4
C
α-FAP
D

A

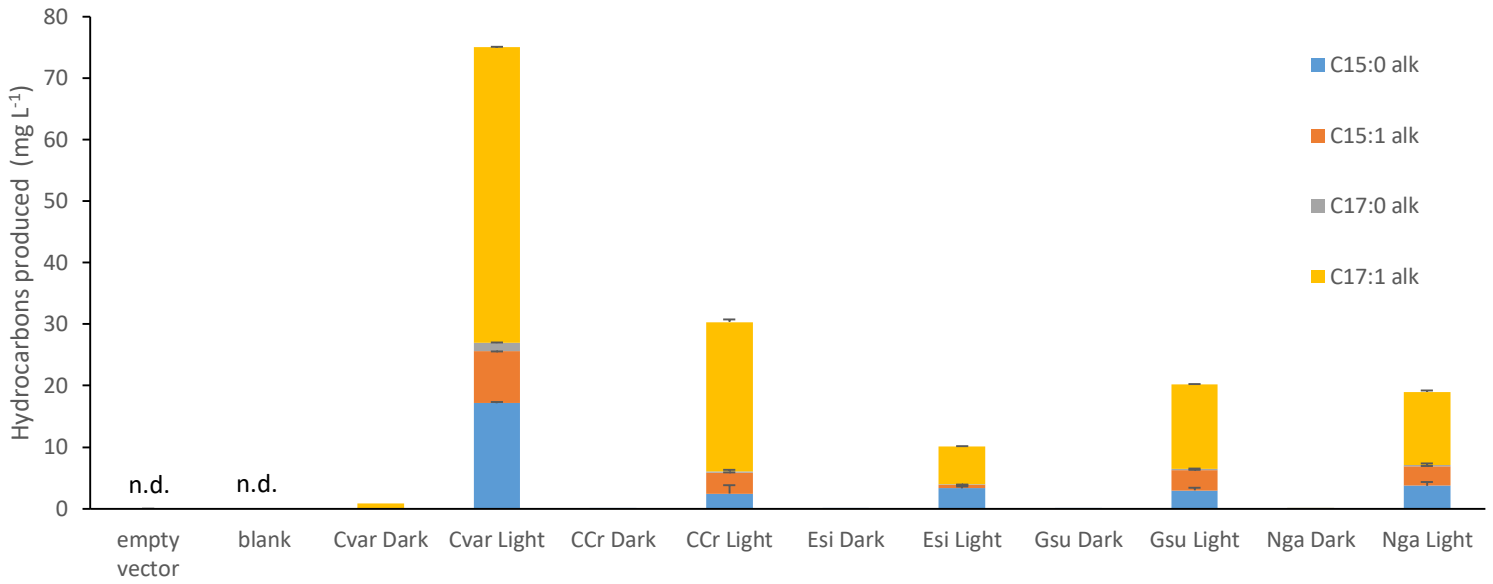
Hydrocarbons produced (mg L-1)
80
70
60
50
40
30
20
10
0
n.d.
n.d.
C15:0 alk
C15:1 alk
C17:0 alk
C17:1 alk
empty vector
blank
Cvar Dark
Cvar Light
CCr Dark
CCr Light
Esi Dark
Esi Light
Gsu Dark
Gsu Light
Nga Dark
Nga Light

B

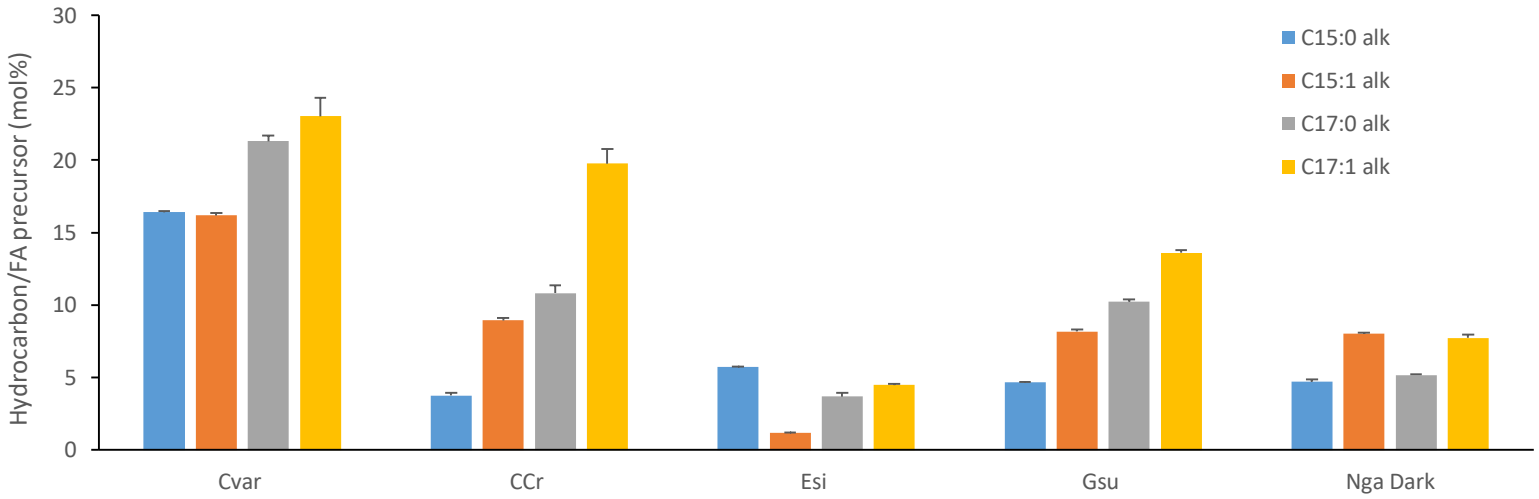
Hydrocarbon/FA precursor (mol%)
30
25
20
15
10
5
0
C15:0 alk
C15:1 alk
C17:0 alk
C17:1 alk
Cvar
CCr
Esi
Gsu
Nga Dark

A

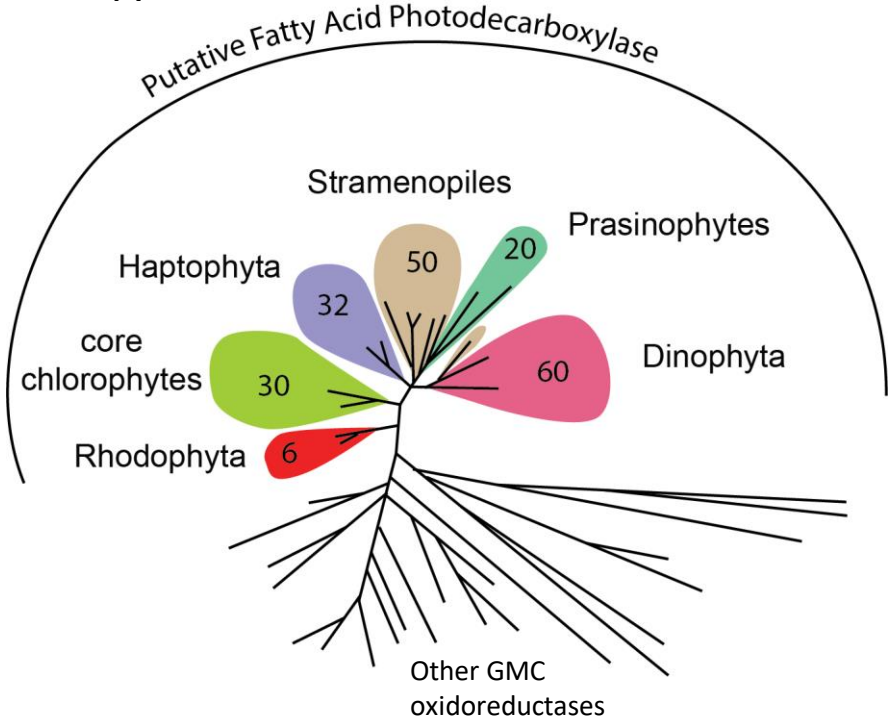

B

Phylum		Species (abbreviation in full tree and name)	
Rhodophyta		*Grc*	*Gracilariopsis chorda*
		Chcr	***Chondrus crispus***
		Pye	*Pyropia yezoensis*
		Pum	*Porphyra umbilicalis*
		Gsu	***Galdieria sulphuraria***
		Cme	*Cyanidioschyzon merolae*
Chlorophyta	core chlorophytes	*Chles*	*Chlamydomonas eustigma*
		Chlch	*Chlamydomonas chlamydogama*
		Vc	*Volvox carteri f. nagariensis*
		Gpe	*Gonium pectorale*
		Cr	***Chlamydomonas reinhardtii***
		Chlle	*Chlamydomonas leiostraca*
		Dus	*Dunaliella salina*
		Chl68	*Chlamydomonas* sp.
		Cso	*Chlorella sorokiniana*
		Mic	*Micractinium conductrix*
		Cv	***Chlorella variabilis NC64A***
		Bbr	*Botryococcus braunii*
		Cs	*Coccomyxa subellipsoidea C-169*
		Lobi	*Lobosphaera incisa*
		Ras	*Raphidocelis subcapitata*
		Chrzo	*Chromochloris zofingiensis*
		Ulmu	*Ulva mutabilis*
		Picsa	*Picocystis salinarum*
		Pic	*Picochlorum* sp.
		Picoc	*Picochlorum oculata*
		Picok	*Picochlorum oklahomensis*
Haptophyta		*Chry*	*Chrysochromulina*
		Ehu	*Emiliania huxleyi*
Heterokontophyta (Stramenopiles)	Bacillariophyceae	*Psm*	*Pseudo-nitzschia multistriata*
		Ptr	*Phaeodactylum tricornutum*
		Frc	*Fragilariopsis cylindrus*
		116393708	*Thalassiothrix antartica*
		116110556	*Corethon pennatum*
	Eustigmatophyceae	*Nga*	***Nannochloropsis gaditana***
		Nsa	*Nannochloropsis salina*
	Phaeophyceae	*Esi*	***Ectocarpus siliculosus***
	Pelagophyceae	*Aa*	*Aureococcus anophagefferens*
Dinophyta		*52837172*	*Neoceratium fusus*
		97429747	*Eterocapsa* sp.
Chromerida		*Chve*	*Chromera velia*

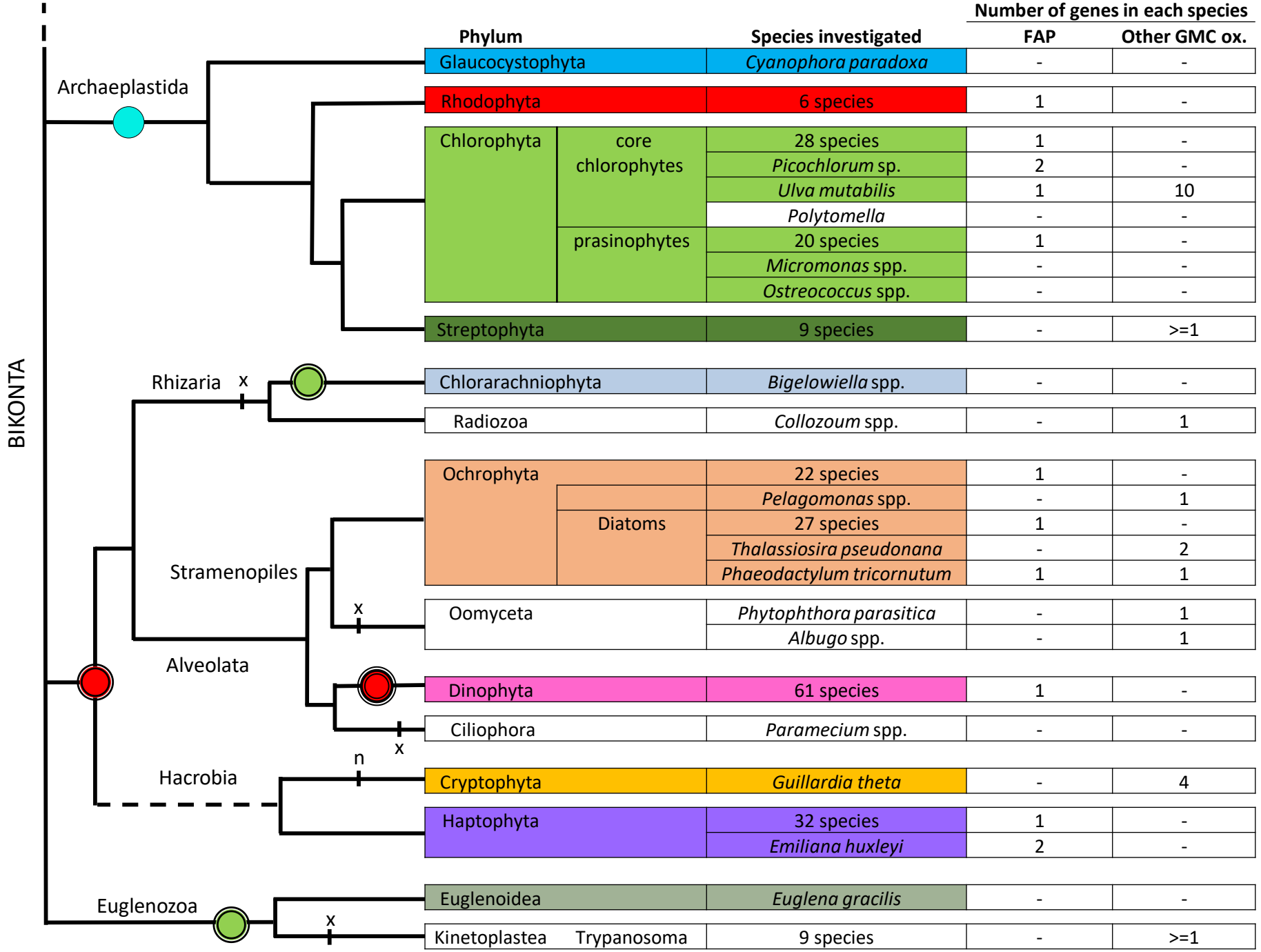

Phylum		Species investigated	Number of genes in each species: FAP	Number of genes in each species: Other GMC ox.
Glaucocystophyta		*Cyanophora paradoxa*	-	-
Rhodophyta		6 species	1	-
Chlorophyta	core chlorophytes	28 species	1	-
		Picochlorum sp.	2	-
		Ulva mutabilis	1	10
		Polytomella	-	-
	prasinophytes	20 species	1	-
		Micromonas spp.	-	-
		Ostreococcus spp.	-	-
Streptophyta		9 species	-	>=1
Chlorarachniophyta		*Bigelowiella* spp.	-	-
Radiozoa		*Collozoum* spp.	-	1
Ochrophyta		22 species	1	-
		Pelagomonas spp.	-	1
	Diatoms	27 species	1	-
		Thalassiosira pseudonana	-	2
		Phaeodactylum tricornutum	1	1
Oomyceta		*Phytophthora parasitica*	-	1
		Albugo spp.	-	1
Dinophyta		61 species	1	-
Ciliophora		*Paramecium* spp.	-	-
Cryptophyta		*Guillardia theta*	-	4
Haptophyta		32 species	1	-
		Emiliana huxleyi	2	-
Euglenoidea		*Euglena gracilis*	-	-
Kinetoplastea	Trypanosoma	9 species	-	>=1

A

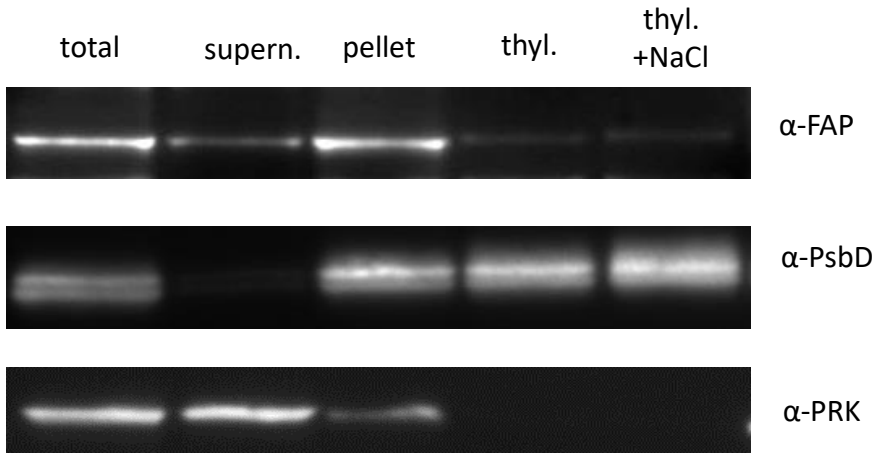
total
supern.
pellet
thyl.
thyl. +NaCl
α-FAP
α-PsbD
α-PRK

B

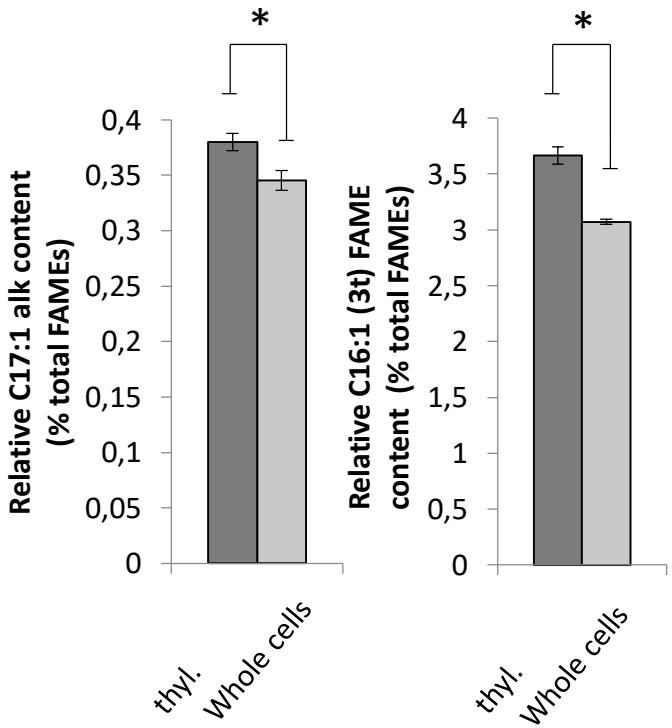
*
Relative C17:1 alk content (% total FAMEs)
0,4
0,35
0,3
0,25
0,2
0,15
0,1
0,05
0
thyl.
Whole cells
*
Relative C16:1 (3t) FAME content (% total FAMEs)
4
3,5
3
2,5
2
1,5
1
0,5
0
thyl.
Whole cells

C

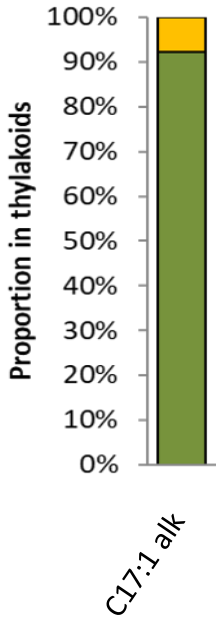
Proportion in thylakoids
100%
90%
80%
70%
60%
50%
40%
30%
20%
10%
0%
C17:1 alk

A

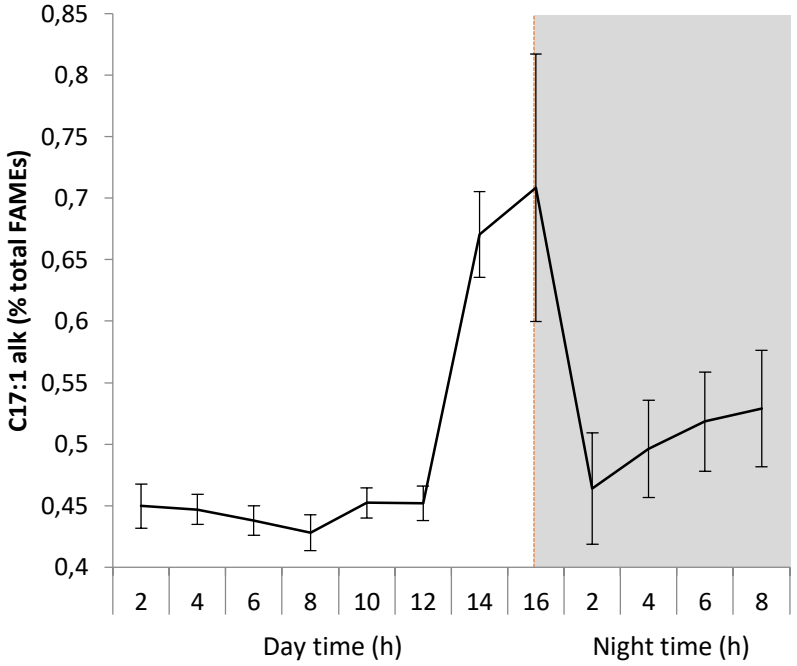
C17:1 alk (% total FAMEs)
0,85
0,8
0,75
0,7
0,65
0,6
0,55
0,5
0,45
0,4
2 4 6 8 10 12 14 16 2 4 6 8
Day time (h)
Night time (h)

B

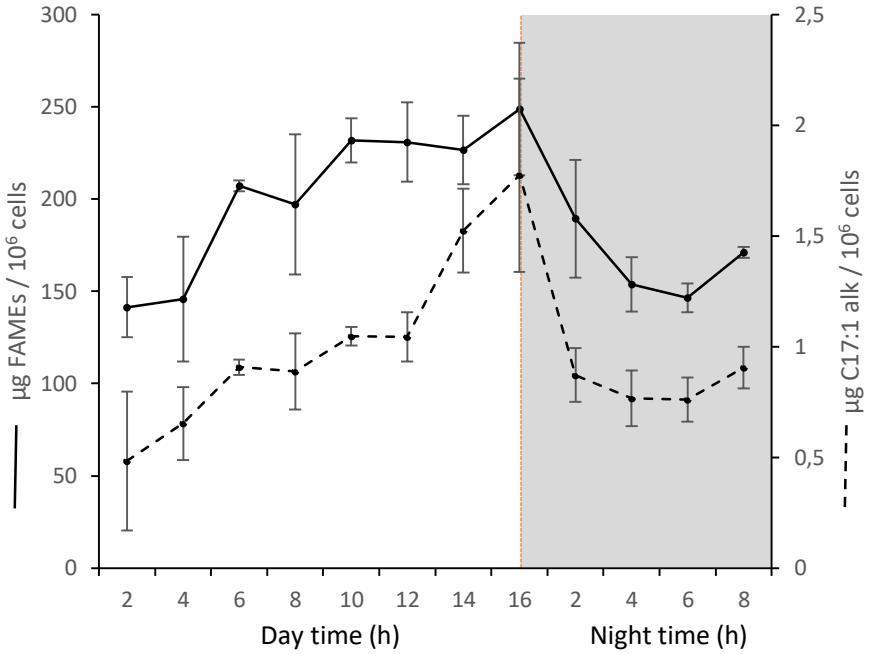
µg FAMEs / 10⁶ cells
µg C17:1 alk / 10⁶ cells
300
250
200
150
100
50
0
2,5
2
1,5
1
0,5
0
2 4 6 8 10 12 14 16 2 4 6 8
Day time (h)
Night time (h)

C

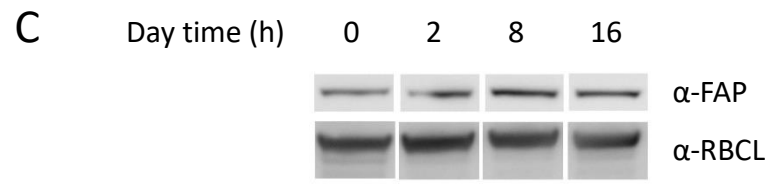
Day time (h)
0
2
8
16
α-FAP
α-RBCL

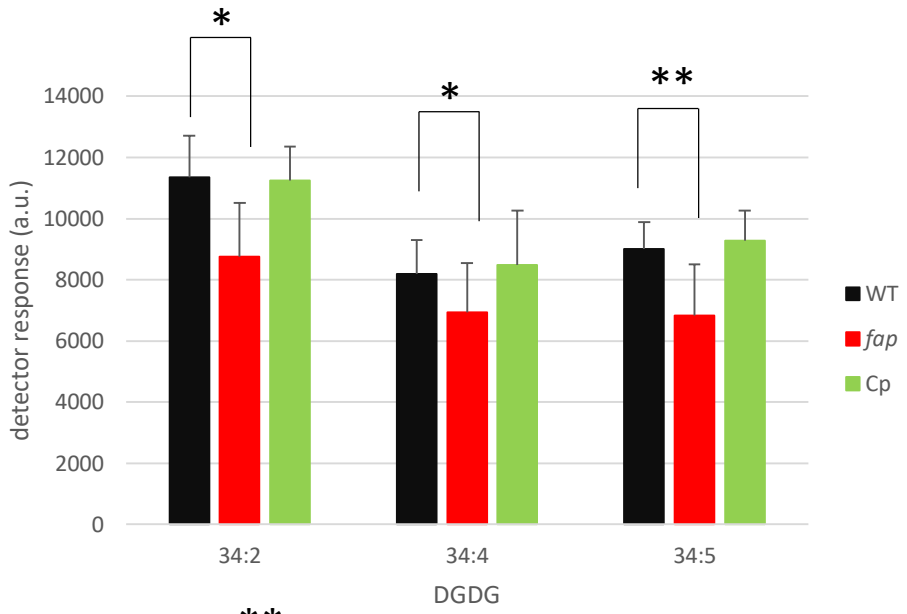
*
*
**
14000
12000
10000
8000
6000
4000
2000
0
detector response (a.u.)
34:2
34:4
34:5
DGDG
WT
fap
Cp

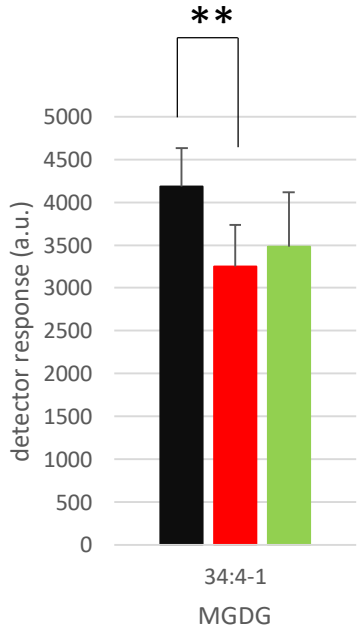
**
5000
4500
4000
3500
3000
2500
2000
1500
1000
500
0
detector response (a.u.)
34:4-1
MGDG

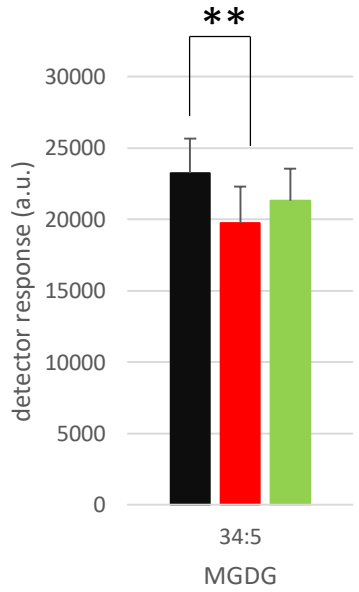
**
30000
25000
20000
15000
10000
5000
0
detector response (a.u.)
34:5
MGDG

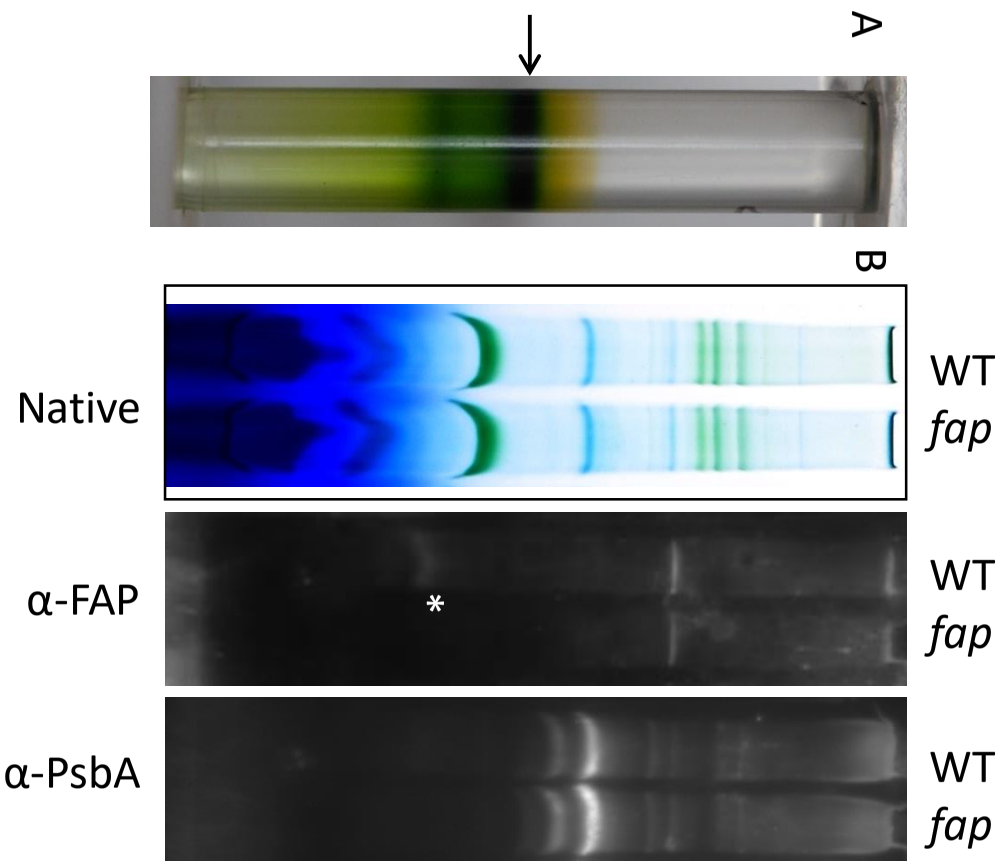
A
B
Native
WT
fap
α-FAP
*
WT
fap
α-PsbA
WT
fap

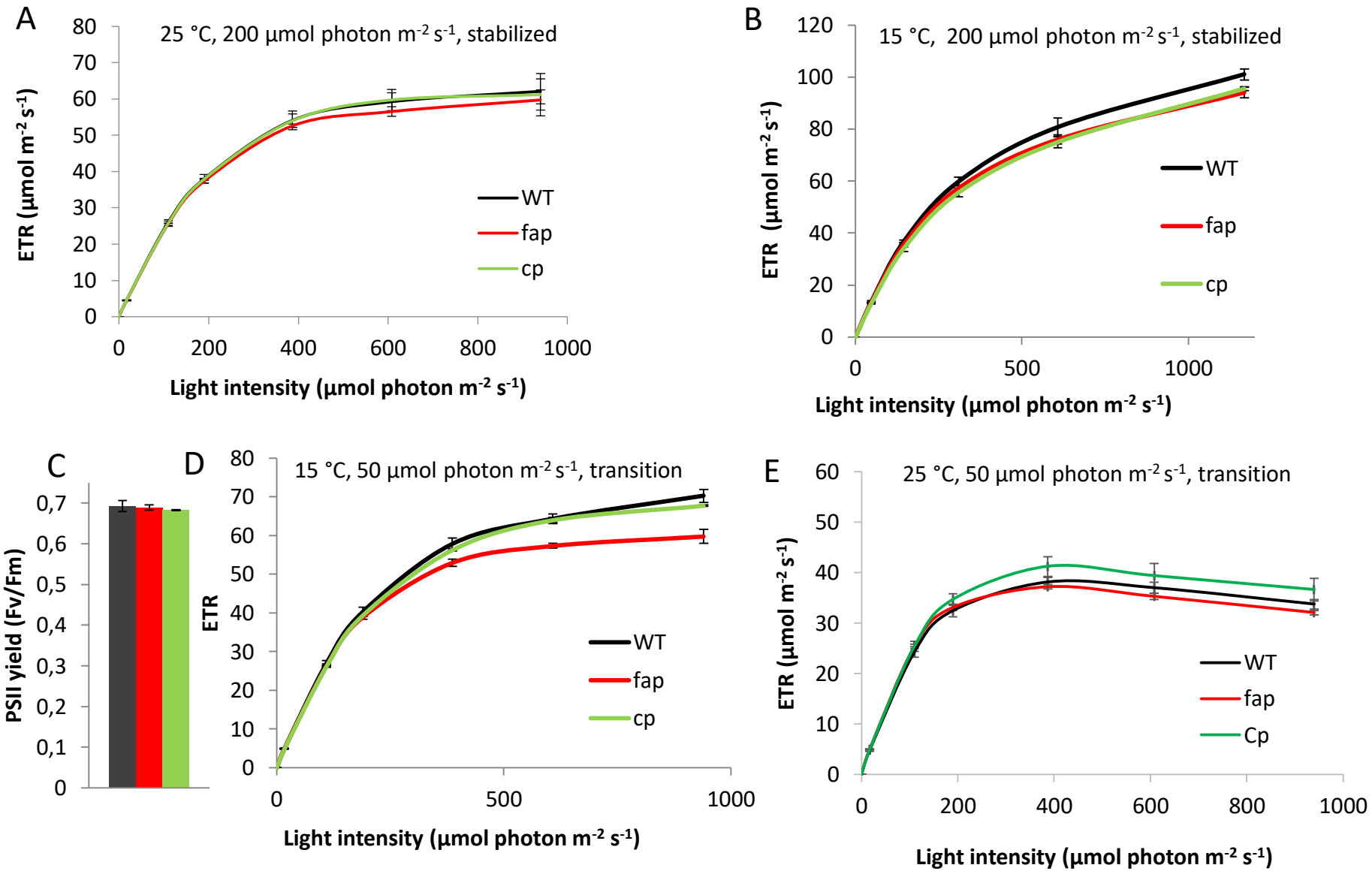
A
25 °C, 200 µmol photon m-2 s-1, stabilized
ETR (µmol m-2 s-1)
Light intensity (µmol photon m-2 s-1)
WT
fap
cp
B
15 °C, 200 µmol photon m-2 s-1, stabilized
ETR (µmol m-2 s-1)
Light intensity (µmol photon m-2 s-1)
WT
fap
cp
C
PSII yield (Fv/Fm)
D
15 °C, 50 µmol photon m-2 s-1, transition
ETR
Light intensity (µmol photon m-2 s-1)
WT
fap
cp
E
25 °C, 50 µmol photon m-2 s-1, transition
ETR (µmol m-2 s-1)
Light intensity (µmol photon m-2 s-1)
WT
fap
Cp

A

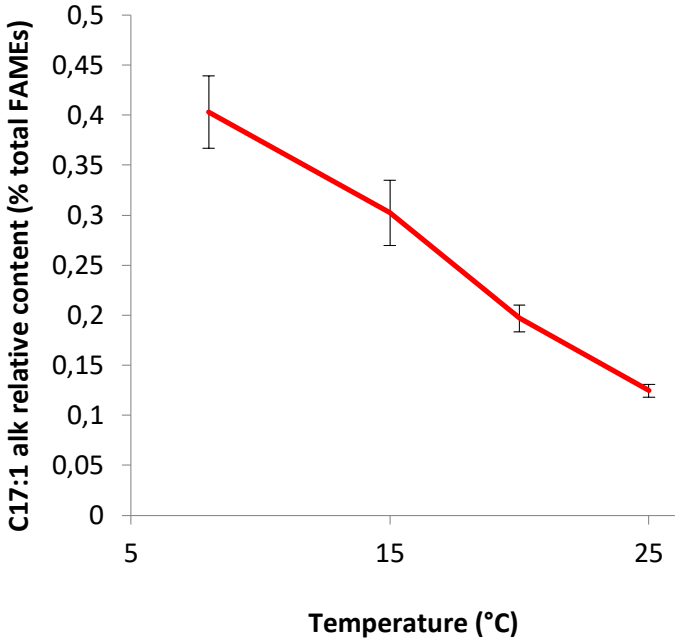
C17:1 alk relative content (% total FAMEs)
0,5
0,45
0,4
0,35
0,3
0,25
0,2
0,15
0,1
0,05
0
5
15
25
Temperature (°C)

B

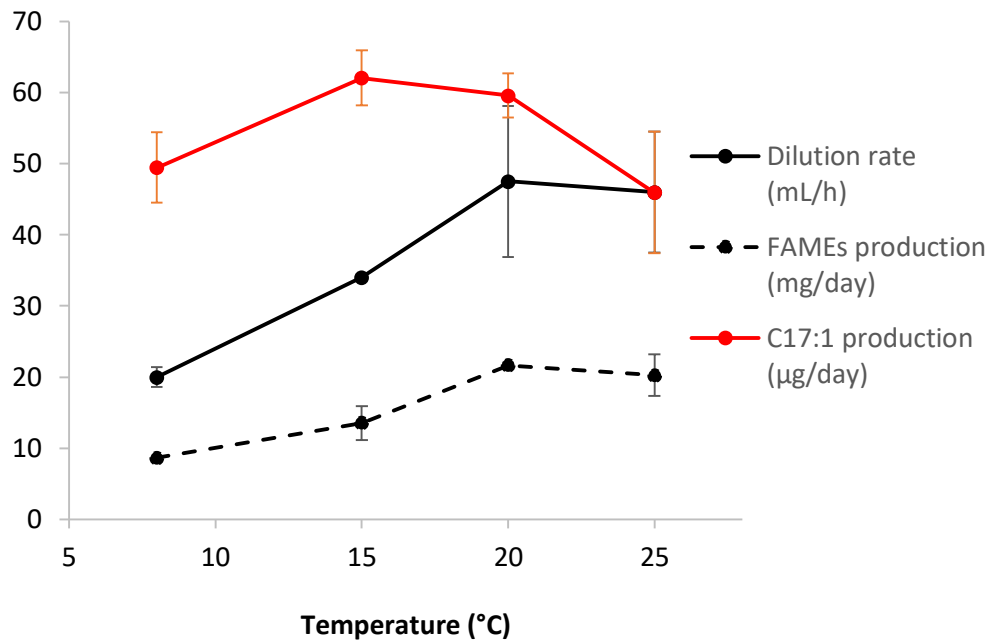
70
60
50
40
30
20
10
0
5
10
15
20
25
Temperature (°C)
Dilution rate (mL/h)
FAMEs production (mg/day)
C17:1 production (µg/day)

cis-vaccenic acid-containing membrane lipid (thylakoids)

Putative lipase

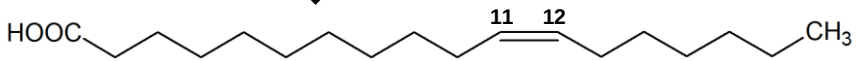

cis-vaccenic acid (C18:1*cis*Δ11)

Blue light

Fatty acid photodecarboxylase (FAP)

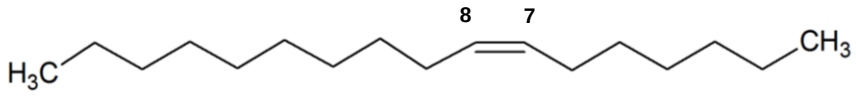

7-heptadecene

Other?

Membrane fluidity, curvature?

Cell signaling?

Direct interaction with specific proteins?